International Energy Agency

IEA District Heating - Annex 4
- Network Supervision

Quantitative Heat Loss Determination by means of Infrared Thermography - The TX model

Heimo Zinko, project leader
and
Johan Bjärklev
Henrik Bjurström
Margaretha Borgström
Benny Bøhm
Lasse Koskelainen
Gary Phetteplace

June 1996

Summary

This report is the final report of the IEA District Heating Project, Annex 4, "Supervision of District Heating Networks. The aim of the project was to further analyze and verify a method developed earlier for determining the heat loss from buried district heating pipes by measuring the temperature profile on the ground surface above the pipes. The temperature measurements can be made by means of infrared (IR) thermography using equipment such as modern IR thermography cameras.

The report describes the work done in the four co-operating countries Denmark, Finland, Sweden and USA for verifying the TX model established in work performed in IEA, Annex 3. The TX model hypothesizes that the temperature distribution on the ground surface above the pipes corresponds - under certain circumstances - to the heat loss from the pipes. By including the major influences of the climate, especially of the wind and the changing surface temperature, we have derived a semi-empirical equation for the heat loss when the TX factor, i. e. the integral of the surface temperature profile across the pipe, is measured. This model is called the advanced TX-interpretation model ATXIM.

Two kinds of investigations have been performed during the verification phase: Simulations and experimental evaluations on test fields.

Simulations have been performed with a finite difference program simulating the heat flow in the ground and between the ground surface and the surroundings. A computer program developed earlier was modified for reading actual weather data based on hourly mean values. The program was used for simulating a multitude of cases with different climate and soil conditions. As a result of these studies we determined that the wind is a very important parameter affecting the TX value. By including the mean wind velocity of the last 7 hours in the ATXIM, the agreement between the simulation and ATXIM could be significantly improved. Other important parameters are the burial depth of the pipes, and the change of the pipe temperatures during the preceding week.

In parallel, experimental evaluation of the TX model was carried out on test fields in the four countries with pipe systems where heat loss was monitored separately. In these test fields in Denmark, Sweden and USA, temperature and energy losses could be monitored continuously, and in some cases also the TX factor could be derived by measurements of the surface temperature profile with temperature sensors. We discovered, however, that IR measurements are the most reliable way of measuring the TX factor. When the ATXIM was applied to IR measurements of the TX factor on the three test fields, and also to a TX evaluation of earlier measurements on a test field carried out in Finland, the result was in reasonable agreement with the heat losses measured in conventional ways.

Hence it can be concluded that under certain well controlled conditions, the heat loss of pipes in district heating networks can be determined quantitatively by analysing the TX profile. The TX profile is best measured using an IR thermography camera, of which there are a number commercially available. The surface must be uniform over the integration width which should be between 3.5 and 5 m. Thermography can be applied at both night and day conditions, but the surface of the test area must have been irradiated uniformly during the last hour, preferably longer. Wet surfaces and rain conditions must be avoided. Grass surfaces and uneven surfaces are difficult to evaluate. If these caveats are observed, it is expected that measurements will achieve an accuracy within ± 20%.

Table of contents

Acknowledgement

This project was initiated and supported by the IEA - District Heating and Cooling Program, Annex IV. However the co-operative work of this project could not have been carried out without the active support by the following national administrations:

District Heating Research Programme, Nordic Council of Ministers

Technical University of Denmark

Danish Energy Agency (j. nr. 1323/93-0027)

National Board for Industrial and Technical Development - NUTEK, Sweden

Chalmers University of Technology, Sweden.

Finnish District Heating Association

US Army, Corps of Engineers, Office of the Chief of Engineers
Military Programs, Washington, DC, USA

The authors wish also to thank Prof. Sture Andersson for his personal support to carry out this project. Furthermore the assistance and advice of the members of the IEA Experts Group (see the preface) is gratefully acknowledged.

Further thanks go to the colleagues and technicians at the participating institutions of Sweden, Denmark, Finland and USA for the most valuable assistance without which our work would not have been successful:

Sweden: Håkan Walletun, Svenn Farvolden, Bengt Perers, Bengt Jönsson and Andreas Nyblom
Denmark: Lars Gullev, Reinhardt Jensen, Henrik Hansen, Odd Brusgaard and Thomas Schmidt
Finland: Veli-Matti Mäkelä
USA: David Carbee, Byron Young and Courtney Eiane

We would also greatly acknowledge the assistance by following experts and companies helping us with IR equipment and evaluation software:

Thomas Perch Nielsen, Danish Technological Institute, Centre for District Heating Technology
Sven-Åke Ljungberg, Royal Technical University Stockholm, Construction and Environment, Gävle
Tomas Jytebrink, AGEMA Infrared Systems AB, Stockholm

Affiliations of the project participants:

Prof. Benny Bøhm
tekn dr Margaretha Borgström
Centre for District Heating Technology
Dept. of Energy Engineering
Technical University of Denmark
DTH Bygning 402A
DK-2800 LYNGBY
DENMARK
Phone: + 45 45 93 1199/40
Fax: + 45 45 93 2166

PhD. Lasse Koskelainen
Helsinki University of Technology
Department of Mechanical Engineering
FIN- 02150 ESPOO
FINLAND
Phone: + 358 0 451 3622
Fax: + 358 0 451 3419

tekn dr Henrik Bjurström
Fjärrvärmeutveckling FVU AB
present address:
ÅF-Energikonsult Stockholm AB
Box 8133
S-104 20 Stockholm
SWEDEN
Phone: + 46 8 657 10 28
Fax: + 46 8 653 31 93

Dr. Phil. Heimo Zinko
Johan Bjärklev
ZW Energiteknik AB
Box 137
611 23 NYKÖPING
SWEDEN
Phone: + 46 155 20 30 80
Fax: + 46 155 21 03 84

PhD. Gary Phetteplace
US Army Cold Regions Lab.
72, Lyme Rd.
Hanover, NH 03755-1290
U.S.A
Phone: + 1 603 646 4248
Fax: + 1 603 646 4640

Preface

This report is the final report of the IEA District Heating Project, Annex 4, ”Supervision of District Heating Networks”. **The aim of the project is the further analysis and verification of a method established earlier for determining the heat loss from buried district heating pipes by means of the temperature profile on the ground surface above the pipes as measured with infrared (IR) equipment.**

The TX model was proposed about 10 years ago and basic analysis was done by researchers at Studsvik Energy (Perers and Schmeling, 1989; Perers and Jönsson, 1990). A more detailed analysis of the TX model was carried out within the IEA - DH&C Program - Annex III and reported by NOVEM (Jönsson, Zinko, 1992). This work was based on field measurements at Studsvik and on a ground simulation model that used finite difference techniques in combination with a model climate. An expert group monitored and supported the work. The results were also tested in a limited field application.

Because of the large interest for a potential quantitative method of heat loss determination based on easily applicable IR technology, it was decided to continue the work in Annex IV within the IEA district heating and cooling Program. It was decided to perform this work as a joint research work with the members of Studsvik’s group (now working in new companies) as project leader and main contractor and the Annex 3 experts from Denmark, Finland and USA as project participants, doing parallel work at their own laboratories. Hence the *Project Group* consists of following participants:

Heimo Zinko, ZW Energiteknik, Nyköping, Sweden (Project leader)

Henrik Bjurström, Fjärrvärmeutveckling FVU AB, Studsvik, Sweden

Benny Bøhm, Lab. of Heating and Air Conditioning, DTH, Lyngby, Denmark

Margaretha Borgström, Lab. of Heat. and Air Cond., DTH, Lyngby, Denmark *)

Lasse Koskelainen, Lappeenranta University of Technology, Lappeenranta, Finland

Gary Phetteplace, US Army Cold Regions Laboratory, Hanover, NH, USA.

*) Margaretha Borgström was working partially in the project within a project extension, see Chpt. 8)

The work of the project group was monitored and supported by an *Experts Group* including following experts:

Chris W. Snoek, CANMET/Energy, Ottawa, Canada
Jens A. Melballe, A/S Bjeld&Lauridsen, Fredericia, Denmark
Veli-Matti Mäkelä, Lappeenrannan Energialaitos, Lappeenranta, Finland
Wilhelm Althaus, UMSICHT, Oberhausen, Germany
Huub G. K. Stroeken, NOVEM, Sittard, The Netherlands
Sven-Åke Ljungberg, KTH Bygg&Miljö, Stockholm, Sweden
Ha Gyoon Chang, Korean District Heating Corporation, Seoul, South Korea
Sharon Semanovich, Allen Applied Infrared Technologies, South River, NJ, USA

1 Introduction

In those countries which have used district heating for many years, a new concern has recently arisen: Certain district heating networks are approaching the end of their technical lifetimes and the heat loss in older piping networks has the potential to increase significantly. In order to chart the requirements and resources for maintenance measures, it is important to be able to diagnose the conditions of the piping network, most importantly the heat losses from the pipes.

Historically, several different methods have been used for determining the heat loss from buried pipes. A survey of these methods is given by Borgström, 1991. The most commonly used method of measuring heat losses from pipes has been to take out a pipe specimen to the laboratory and to measure the heat loss in a controlled steady-state experiment. Such type of measurements of different types of pipe systems including water pipe, insulation and outer casing has been performed by Carlsson et. al. 1963. In these experiments, temperature sensors and water flow meters were used for determining the overall heat loss from the pipes. Jonasson,1986, has performed measurements on prefabricated joint pipes by essentially measuring the temperature difference between distribution water and pipe casing, together with air and ground temperature, by means of thermocouples and comparing the results with theoretical expressions fitting the right set of parameters. Phetteplace et al., 1991, has conducted field experiments comparing several methods of measuring heat losses on operating systems. Benny Bøhm, 1990, introduced heat flux meters for measuring the heat loss from buried pipes and compared these results with results calculated from the measured temperature distribution in a section perpendicular to the pipe. The problem of heat flux meters has been attributed to their calibration with the surrounding (unknown) ground properties. Margaretha Borgström, 1994, made a very detailed study of the heat loss from prefabricated pipes by means of heat flux meters. In this case however, the pipes were locally uncovered from all soil and hence the surrounding media was air and a well known shielding insulation.

One other method increasingly used for qualitative heat loss detection and status control of district heating networks is based on airborne and ground borne thermography. In this method the mapping of the ground temperature can be used to give qualitative information about the network condition, mainly with the aim of finding leaks (Bartsch, 1979; Ljungberg, 1987; Hansen, 1987). These techniques rely primarily on relative changes of the temperature pattern along the pipe.

With the help of more refined analytical methods it should be ultimately possible not only to trace leaking media pipes, but also to determine the condition of the insulation. In the quantitative heat loss analysis, it is presumed that the temperature profile on the ground surface above the pipes, measured in the direction perpendicular to the pipe alignment, is related to the pipe heat loss. The basic idea is that the integral of the temperature variation across the pipe, called TX, is a function of the heat

loss. Obviously TX is also affected by other parameters such as depth, heat diffusivity of the ground and so on. By including all of these parameters in an interpretation model it is proposed that one may determine the amount of heat loss quantitatively and hence to draw conclusions about a potential damage to the protective casing or the pipe (Perers, 1989; Perers and Jönsson, 1990). Figure 1 illustrates this basic idea.

Figure 1.1 Thermography of buried district heating pipes and the TX-profile.

A more detailed analysis of the TX model was carried out within the IEA - DH&C Program - Annex III and reported by NOVEM (Jönsson, Zinko, 1992). The analysis was based on field measurements at Studsvik and on a ground simulation model that used finite difference techniques in combination with a model climate. The results were also tested in a limited field application.

In addition to a physical description of the pipe and of the surrounding ground, the finite element model includes freezing and evaporation of water in the ground and on the surface, solar radiation, snow, rain, condensation, convection, wind, and the exchange of IR radiation between the ground and the atmosphere and the surroundings, respectively, see Fig. 3.2. However, the interpretation model - called TX-model was derived for a limited set of conditions corresponding to variations of some of the parameters discussed above.

The objective of this phase of the project is to further develop and verify the method of IR heat loss evaluation on district heating pipes by means of the TX-model to determine its potential and limitations for determining the status of pipes and its possible use for planning service and maintenance on the network.

The work which has been carried out includes the following items:

- Installations of test sites for TX-measurements in different countries
- Modelling of test-sites with the ground model simulation program
- Experimental verification of the model with test-field results
- Refining the model by systematic sensitivity studies
- Application of the TX model in IR field surveys

2 The heat transfer from buried pipes

2.1 HEAT TRANSFER FUNDAMENTALS

The heat loss from buried pipes under steady-state conditions can be theoretically determined starting with a pair of pipes at different temperatures T_f and T_r respectively. Other factors that need to be known are burial depth, thermal conductivity of ground and pipe insulation, ambient temperature, and the geometrical parameters of the pipes. For the most common case of two buried pipes the heat loss can be determined by the following equation (1):

$$Q = \frac{2\left(\frac{T_f + T_r}{2} - T_o\right)}{\frac{\ln\left(\frac{D}{d}\right)}{2\pi\lambda_i} + \frac{\ln\left(4\left(\frac{H + D/2}{D}\right)\right)}{2\pi\lambda_m} + \frac{\ln\left(2\left(\frac{H + D/2}{S}\right)^2 + 1\right)}{4\pi\lambda_m}} \qquad (1)$$

$$H = h_f + \lambda_m / \alpha$$

with

Q = heat loss per m double pipe system, W/m
T_f, T_r = feed and return temperature, respectively, °C
T_0 = undisturbed soil temperature, °C
λ_i = heat conductivity of the insulation, W/(m·°C)
λ = heat conductivity of the surrounding ground, W/(m·°C)
D, d = outer and inner radius of insulation, m
h_f = buried depth of pipe, m
S = distance between pipes, m
α = convective heat transfer coefficient between surface and air, W/(m²·°C)

(see also Figure 2.1)

The heat loss Q from a single, buried pipe can, according to (Bøhm, 1990), from equation (1) be derived as following:

$$Q = \frac{2\pi \cdot \lambda_s \cdot \Delta T_s}{\ln\left(1 + 2\lambda_s / (\alpha \cdot h_f)\right)} \qquad [W/m] \qquad (2)$$

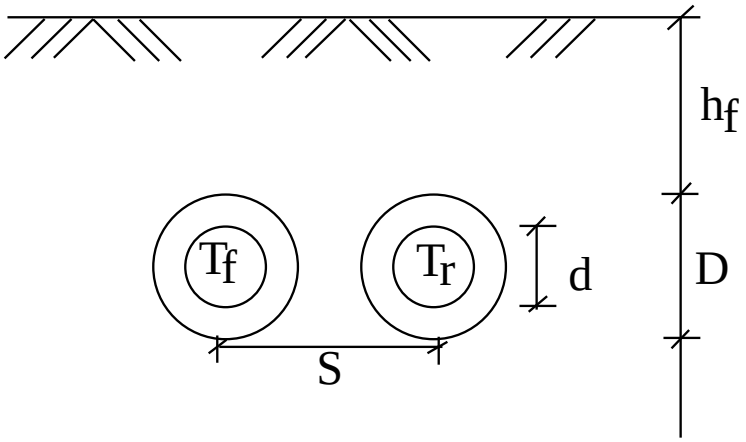

Figure 2.1: Parameters for determination of the heat loss of buried pipes.

where
ΔT_S = temperature difference between ground surface and pipe surface.

For small values of the logarithmic argument, equation (2) simplifies further to

$$Q \approx (\pi \cdot \alpha \cdot h_f) \cdot \Delta T_s \qquad (3)$$

The surprising result of Equation 3 is that in the first approximation there is no influence of the thermal conductivity of the soil on the heat loss and that the overall influence of the ground thermal conductivity on the temperature profile on the soil surface and hence on the TX factor might be small under steady state conditions. On the other hand, the convective heat transfer coefficient and therefore the wind conditions will play an important role for the determination of heat losses from surface conditions.

However, in the case of non steady-state conditions, i.e. if the pipe temperatures varies because of changing load conditions, the expressions becomes more complicated because of the heat capacity of pipe and ground material. In this case a dynamic model must be used in order to relate temperature differences to heat loss coefficients. In general terms, the propagation of isotherms can be described by a thermal diffusivity *a* which can be derived from Fourier's law (4) and a local energy balance (5).

$$Q = -\lambda_m \nabla T \qquad (4)$$

$$C_m = \frac{\vartheta T}{\vartheta t} + \nabla \cdot Q \qquad (5)$$

Equation (4) and (5) result for constant material parameters λ_m and C respectively in the following equation (6):

$$\nabla^2 T = \frac{1}{a} \cdot \frac{\vartheta T}{\vartheta t} \qquad (6)$$

with
C_m = volumetric heat capacity of the ground, J/(m³·°C)
a = λ / C_m = heat diffusivity, m²/s

For example, it can be shown (Hellström, 1991) that the characteristic penetration depth d_p for a periodic thermal process such as the daily change of the ambient temperature into the ground is

$$d_p = \sqrt{a t_p / \pi} \approx 0.08 \quad [m] \qquad (7)$$

with t_p = period time = 86400 s and a = $2.5 \cdot 10^{-7}$ m²/s for typical ground conditions.

Hence the influence of the daily change in climatic conditions is primarily expected to be limited to the upper layer immediately below the ground surface. On the other hand, changes of the heat distribution media temperature and the resultant heat loss from buried pipes can be expected to take several days before being detectable at the surface as changes in the surface temperature distribution.

2.2 THE TX FACTOR PRINCIPLE

The TX factor method for quantifying the heat losses from district heating pipes is based on the temperature distribution at the ground surface above the pipes. In early experiments a correlation between the temperature profile at the ground surface perpendicular to the pipes and the heat loss was observed (Perers and Schmeling, 1989). The area below the profile is the so called TX factor and is related to the heat loss (see Figure 2.2). Mathematically the TX factor is expressed as follows:

$$TX = \int_{-x_m}^{x_m} [T(x) - T(x)_{min}] dx \qquad (8)$$

Here:

x_m = Position at the ground surface across the pipes, m

$T(x)$ = Local temperature, °C

$T(x)_{min}$ = The lowest temperature at the ground surface within x_m metres from the centre of the pipes, °C.

Figure 2.2 The variation of the TX profile for a sunny day.

By using the lowest temperature T_{min} in the profile as reference, the TX factor for all profiles in Figure 2.2 has about the same value (within ca. 10 %).

The measured TX factor is then used to calculate the heat loss by means of the ***interpretation model.***

The interpretation model proposed in Annex 3 (Jönsson, Zinko, 1992) reads:

$$P_f = TX \cdot [A + B \cdot h_f + C \cdot \lambda + D \cdot (dT_m/dt) + E/x_m] + F \cdot h_f + G \cdot \lambda + H \cdot (dT_m/dt) + I/(x_m)^2 \quad (9)$$

The constants A - I were determined by a series of simulations using a numerical model. The interpretation model was then determined from the results of these simulations using a first order multiple regression. In the present study the objective was to adjust the interpretation model such that it would more closely model the observed daily variations of TX. The result is the following proposed ***advanced interpretation model (ATXIM):***

$$P_f = TX_{meas} \cdot [\, 2.5 / (1.34 + 2.35 \cdot (0,8)^{<wind7>}) \,] \cdot [-13.6 + 19.6 \cdot h_f + 4.3 \cdot \lambda + 12.8 \cdot (dT_m/dt) + 40.1/x_m] + 9.1 \cdot h_f - 6.3 \cdot \lambda + 18.8 \cdot (dT_m/dt) + 24.7/(x_m)^2 \quad (10)$$

The TX method requires very high precision in relative temperature measurements. The resolution of the infrared camera is less than 1/10 of a °C for relative temperature measurements, and that is important for this method. This means that the precision in the measurements (and thus the TX factor calculation) depends on the difference between the highest and lowest value in the temperature profile. This difference can be as low as about 0.5 °C, but with our method using relative temperatures measured by a IR camera the accuracy of the measurements can remain relatively high. Thus the method is most accurate where relatively high temperature differences exist such as for pipes with higher heat losses or for pipes buried at shallow depth. We estimate that the model is applicable to pipes buried at depths between 0.5 and 2.0 m.

It should be noted that the TX model is useful only under steady-state or quasi steady-state conditions with respect to the heat flow in the space between the ground's surface and pipe system. The daily climate change affects only the uppermost layer (a few cm) below the surface and is expected to have only a second order influence on the ATXIM (see Chapter. 6 for more details). In a first approximation it can be shown that the temperature profile representing the heat loss is superimposed on the temperature swing of the uniformly heated (or cooled) ground surface temperature following the daily climate variations.

However, there are many parameters affecting the temperature distribution and hence TX which should be included in the ATXIM. Most of the theoretical work attempted to include these parameters and events in order to increase the understanding of the TX model. For the experimental work we tried to avoid such cases in order to get "clean" data unbiased by disturbing events. Among the disturbing influences are: rain and drying surfaces, snow, partial shadowing, and strong varying winds. In Chapter 4, a more detailed account on these effects is given.

3 The simulation program

The simulation program has been developed in order to get a detailed understanding of the heat transfer processes between the ground surface and the buried pipes. The program consists of two parts: **the ground model and the surface model**. The models are based on the finite difference method with different time intervals.

Originally the program was developed with a climate model included. This model was valid for countries with moderate climate based on long term trends in climate variations. For the present Annex 4 work the model has been modified for optional input of any climate defined on a hour by hour basis.

3.1 THE GROUND MODEL

The program simulates a cross section of the ground according to Figure 3.1. The area included in the calculation must be large enough to get an undisturbed ground temperature field at the edges of the area. The thermal properties of the surface material (asphalt, grass, etc.) must be specified in the input data.

Figure 3.1 Geometrical model for the cross section perpendicular to the pipe alignment.

The calculation area is then divided into cells. The cell dimensions might be of different size with small units where large gradients are expected and vice versa. The heat flow between the cells is assumed to be two-dimensional, but for the calculations we assume an unit length of one meter in the direction of the pipes. Two of the cells represent the pipes.

The properties which must be input to the program are:

λ thermal conductivity, W/(m·°C)

C volumetric heat capacity, J/(m³·°C)

x_i, z_i dimension of each cell, m

T initial temperature, °C

R thermal resistance at cell interface, (m²·°C)/W

The model can calculate the heat flow in two dimensions, including also the heat transport by phase change when freezing or evaporation occurs in the ground or at the surface. Of course also radiation exchange with the the surroundings is included.

Freezing and thawing conditions lead in general to very large TX fluctuations. Such conditions are ***not*** suitable for the TX interpretation. For details see Jönsson, Zinko, 1992.

3.2 THE SURFACE MODEL

The most important model for this application is the surface model. The different modes of heat transfer that act at the ground surface can have a large effect on the temperature profile. Therefore it is very important to take into account all the significant modes of heat flow which are acting on the ground surface (see Figure 3.4). The dominant modes are:

- Convection (natural and forced due to wind)
- Latent heat transport (evaporation, condensation, frost)
- Solar radiation (solar absorbtance)
- Long wave radiation (calculated with regard to shielding from the horizon, cloudiness, surface material, moisture, frost and snow)
- A model for snow and water which takes into account the continuously varying layer at the ground surface.

Figure 3.2 Energy balance model including heat flows between the surface and the ground.

Hence a detailed simulation of the heat balance on the ground surface needs the following input data:

- Wind speed, m/s
- Ambient temperature, °C
- Relative air humidity, %
- Rain and snow, mm
- Long wave radiation, W/m²
- Global solar radiation, W/m²

In the simulation program, these variables can be input in different ways: With an synthetic climate included in the program or a real climate to be input as a hour-by-hour data file.

a) Synthetic built-in climate

All the climatic data and the temperatures in the pipes are input as monthly mean values. The program then calculates instantaneous mean values using idealized

shape-formulae according to meteorological experience for the respective parameters.

The wind speed of the synthetic climate model varies in a sinusoidal form with the maximum value at 3 p.m. and minimum value at 3 a.m. The ambient temperature varies in a similar way as the wind speed, but with one oscillation with the period of one month and another oscillation period of 24 hours.

From the wind speed, the ambient temperature, and the surface temperature, the convective heat loss can be determined.

With regards to the influence of rain, the input is the number of days with rain during the month and an assumption of the amount of water remaining after a shower of rain. The latent heat transport due to the evaporation of the water is then calculated using the thermodynamic laws of evaporation and mass transfer.

In the winter, the surface temperature is greatly influenced by the occurrence of snow. The snow affects the surface both as an insulation layer and by its ability to store latent heat. The model works with two cases: Either a constant layer or a melting layer of snow. The number of snowfall periods during the winter and the amount of the fallen snow are required input data.

The long wave radiation is determined by means of the Stefan-Bolzmann law. The sky temperature for a clear sky can be calculated by means of the air pressure and the temperature. The temperature of the cloudy sky is assumed to be 1°C less than the ambient temperature as it was determined from the evaluation of climatic measurements. The background and surface emissivity must be defined in the input file.

The heat transfer due to solar radiation is determined by a simple model including the global solar radiation and the solar absorbtance at the surface. The models for solar and long wave radiation also includes compensation for shading effects.

Starting with a set of initial conditions, the program recalculates the heat balance with time steps between 5 and 30 minutes throughout the year. From this the temperature distribution as well as heat flow through the ground and hence TX factors and can be determined. Thus by using this simulation model, the influence of different parameters such as soil thermal conductivity, pipe dimensions, snow surfaces, etc. can be determined.

b) Real climate input

The second method of inputting climatic data to the program is the direct input of measured hour-by-hour data. Such data are now available for many places in most countries. This method of data input gives a more realistic representation of weather variation with location and hence leads to a better simulation of the heat transfer problem and the resultant TX profile. On the other hand, the real weather data rep-

resent also a very challenging test of a TX model because of the weather conditions can change very rapidly over a wide range. Hence, in principle, it should be possible to compare the theoretical with measured TX values for a test site if all needed climate parameters are measured at the same time.

When actual climatic data are used the input parameters are essentially the same as for the synthetic climate but on a hourly basis. Two parameters turn out to be more critical than the others:

The *long wave radiation* is next to the solar radiation the largest heat flux and hence important to be known relatively well. On the other hand the local long wave radiation might differ quite a lot from that measured one due to local conditions as ground absorbtance, reflections, shading and radiation from surroundings. Hence the net heat flux due to long wave radiation might be difficult to be estimated.

Rain and snow precipitation can be measured, but it is uncertain, how much humidity is left on the surface and what amount entered the ground. Therefore if precipitation is included, an estimate of these quantities must be made which yields some uncertainty in the simulations. Hence a direct comparison with measured values can be only done during dry periods. Also, dew and night humidity can lead to considerable differences between measured and calculated values for TX at any particular time.

On the other hand, the simulations can very well explain overall trends for the daily and seasonal variations of the TX factor. Figure 3.3 a - g show how the temperature distribution between the pipes and surface vary during a day. The calculations are made for a sunny day in June, based on the measured climate of Stockholm 1986. The geometry is that of Figure 3.1 based on the test field of Studsvik with uniform ground conditions and asphalt surface. We call this case **the reference case.**

The Figure 3.3 a shows the actual geometry with horizontal pipes, the asphalt layer in top. The cross section is 10 m width × 5 m depth. To the left, the isotherms in a two-dimensional cross section are shown. To the right, a three-dimensional temperature mountain is added to the isotherms. The Figures 3.3 b to 3.3 g show the temperature changes in for hours intervals starting at midnight, the Figures are turned by 90°. The "top" of the temperature mountains indicates the temperature of the pipe surface in the ground. The Figures illustrate how the temperature of the top layer changes at a sunny day. In the night the asphalt temperatures are lower and a temperature ridge develops some 10 cm down in the ground. With increasing sun, the surface temperature increases reaching a maximum in the afternoon and cools down again at night. The TX profile can easily be seen in the surface layer (to the right of the "mountain top"). Figure 3.4 shows the variation of the TX factor during the same day. The total variation of TX is about ± 15 % during this period, i. e. relatively low inspite of a strong change of irradiation during the day.

Figures 3.3 a-c Temperature distribution in a crossection of the ground around district heating pipes. See explanation in the text.

Figures 3.3 d-g Temperature distribution in a crossection of the ground around district heating pipes. See explanation in the text.

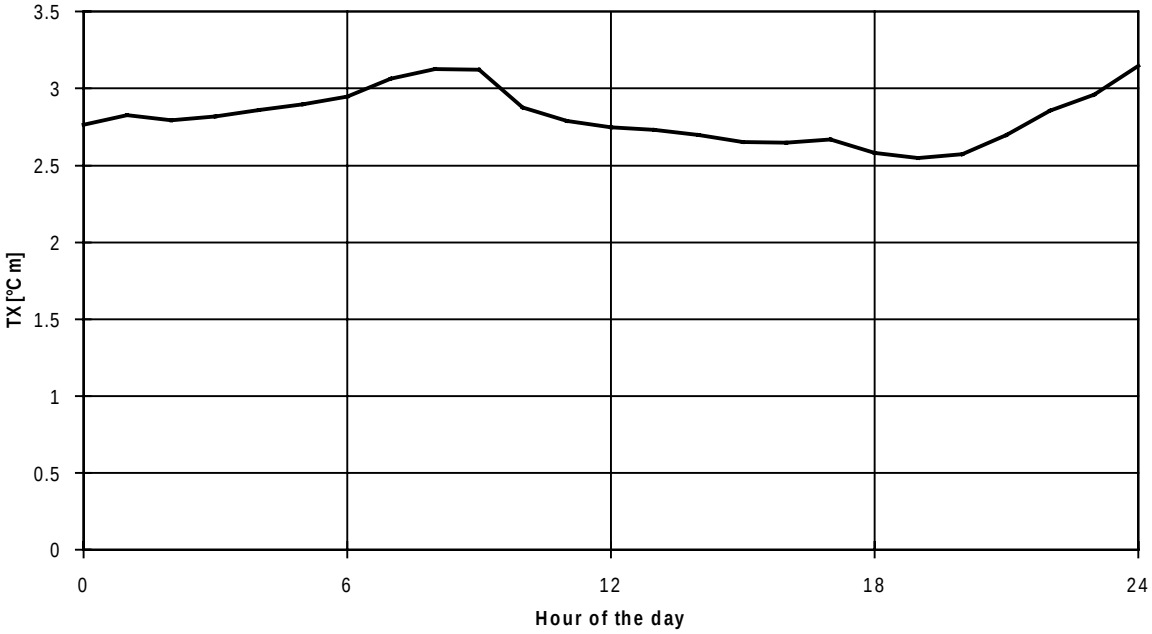

Figure 3.4: TX factor variation for the same day.

4 Simulation results

4.1 ANNUAL SIMULATIONS

The simulation program based on hourly data was used for making long term simulations of the TX factor. The basic configuration was that of the test field in Studsvik according to Figure 3.1. As climate input we used a climate file based on hourly values for Stockholm for 1986 as it is distributed by the Swedish Meteorological and Hydrological Institute (SMHI). The data file contains results from one of a series of measured weather climate data from meteorological stations based on hourly mean values. The data are checked, completed and if necessary corrected. The data are in common use for solar energy calculations.

The following climate data are read by the TX-simulation program:

- Global radiation on a horizontal surface
- Ambient temperature
- Wind velocity
- Infrared radiation
- Air humidity

The other major inputs that are required are the thermal properties of the soil. In our basic calculations we used the following soil properties assumed to be homogeneously distributed in the total soil volume: Thermal conductivity = 1.5 W/(m·K); heat capacity = $3.0 \cdot 10^6$ J/m³.

One disturbing factor in the simulations - as in reality - is the rain. This results from the difficulty discussed earlier regarding the determination of how much water remains on the surface during and after a rain period. The drying process could take several hours or even several days disturbing the resulting TX-factor. Because of the uncertainty in its analysis we circumvented the problem of rain by not including it in the analysis. ***Hence the results are valid for dry periods only.***

The simulations are straightforward and can be performed on a PC. Starting from a uniform isothermal soil temperature distribution, the simulations were repeated for a number of years. The simulation of each subsequent year begins with the temperature distribution in the soil from the end of the preceding year as its initial conditions. After two simulated years, the soil volume of 54 x 25 x 1 m³ is essentially in thermal balance with little or no change of the initial conditions when adding more simulation years. Figure 4.1 shows the variation of the TX factor, the ground temperature and the pipe temperature for the reference year Stockholm 1986 over the entire year. These calculations assumed that the heat loss was constant 54 W/m, see

Figure 4.1. The plots show the large variations of the TX factor when the ground is frozen and a relative constant TX factor during the summer period in spite of vary-

Figure 4.1 Annual simulation for the test field in Studsvik, climate Stockholm 1986. P = 54 W/m, constant heat flow. TX factor, ground temperature and pipe temperature are shown.

Figure 4.2 Annual simulation of the TX factor for the test field in Studsvik, climate Danish reference Year. P = 54 W/m, constant heat flow.

ing ground temperature. The larger fluctuations ("spikes") during the summer and autumn are caused by heavy winds. A more detailed annual plot of the TX factor for 12 months of the year 1986 - Stockholm is shown in Appendix A.

As it can be seen, two main periods can be discerned: One period is the winter period between November and April, in which the TX factor has large variations. The other is the summer period for which the TX fluctuations are much smaller. The reason for the difference is the freezing of the ground. The latent heat effects can effectively disturb the local heat flows and the resulting temperature profiles (for the same reason we excluded the humidity in the ground). ***Hence the TX factor can not be used as a reliable measure for the heat loss if freezing of the ground occurs.*** These conditions are prevailing in South Sweden for almost 6 months, from November until April inclusively.

This fact is also supported by performing the simulations for the same field conditions but with a climate file representing the New Danish Reference Year (Møller Jensen, J. and Lund, H., 1995), see Figure 4.2. By comparing both runs it can be seen that the general trends are about the same, with the only difference that the winter period with large fluctuations due to ground freezing is much shorter in Denmark than in Sweden.

Figure 4.3 TX factor (daily means) and heat loss from pipes with varying average pipe distribution temperatures according to demand control strategies. Synthetic climate for Stockholm.

It should also be noted from the plots in Figure 4.1 and 4.2 that there is strong daily variation of the TX factor. This results from the effects of wind, as it will be explained in Chapter 5.

From Figure 4.1 we can also see the annual change of the pipe temperature and the ground surface temperature. As the simulation was done with constant heat loss from the pipe, the mean temperature difference between the pipe and the ground surface is expected to be essentially constant. In Figure 4.3 another example is shown. Here the hot water distribution temperature and hence the heat loss from the pipes are decreased during the summer period as it is the case in operating district heating networks. Only daily means are plotted for the TX factor. From this figure it can be clearly seen that the TX factor also decreases during the summer period as expected.

4.2 NON UNIFORM GROUND PROPERTIES

The simulations in Chapter 4.1 were performed for completely homogeneous ground conditions. This of course is very rarely the case. However, in many cases otherwise quite suitable for our purposes, the ground conditions might resemble those shown in Figure 5.1. The pipes are buried in a well defined sand bed which is surrounded by the natural soil which might be sand, clay, moraine, gravel or a stone bed. The cover of the ground surface could be asphalt, concrete, sand, or in a worse case, grass. As long the individual layers are reasonably broad, i. e, broader than the TX integration

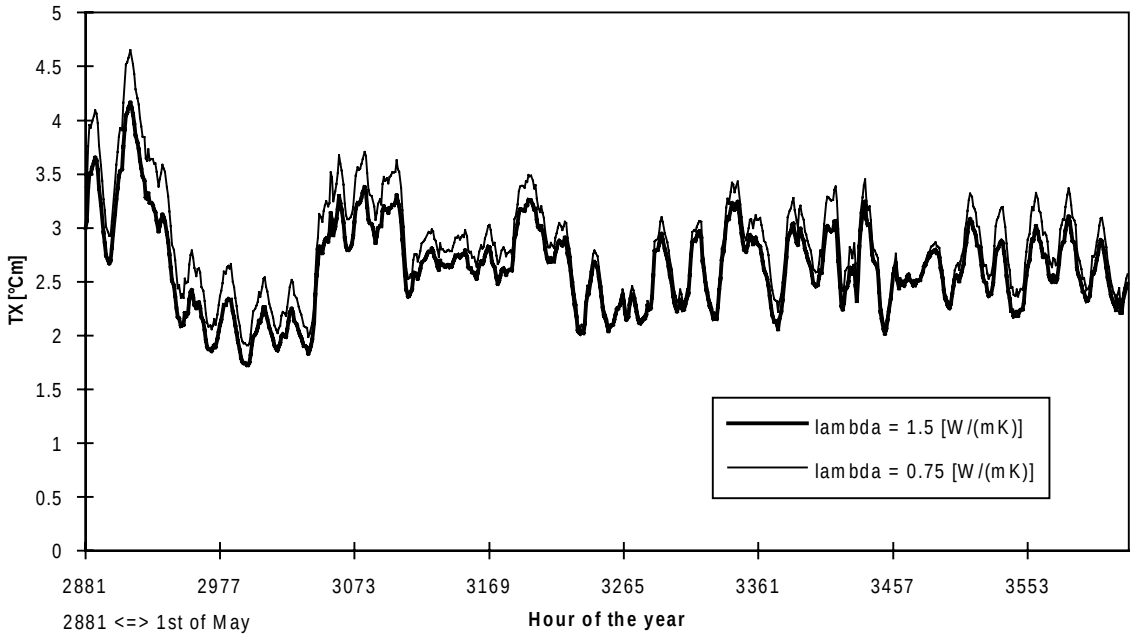

Figure 4.4 Comparison of TX simulation with different heat conductivity in the sand bed.

limits, the TX factor is not heavily affected or disturbed by different physical properties of each layer. Hence a sandbed around the pipes with a thermal conductivity differing from the surrounding soil does not severely impact the TX factor. This is shown in Figure 4.4 for a condition where the heat conductivity of the sand bed is one half that of the surrounding soil including the surface

On the other hand, if the upper most layer near the ground's surface is nonuniform, the TX factor might be more severely impacted and thus a quantitative heat loss analysis might fail. This is shown in figure 4.5. This Figure shows the TX profile at 6 different times of the day for the worse case of different conditions in sand bed, soil, fill and asphalt respectively (see inserted sketch in the Figure 4.5). It should be noted that the x-axis of profile is not in a geometrical scale, instead it is plotted with constant width for each node. In the program, the width of the nodes decreases strongly from outside toward the center of the field. The vertical lines indicates the integration width of 4,5 m, the total field width is 54 m.

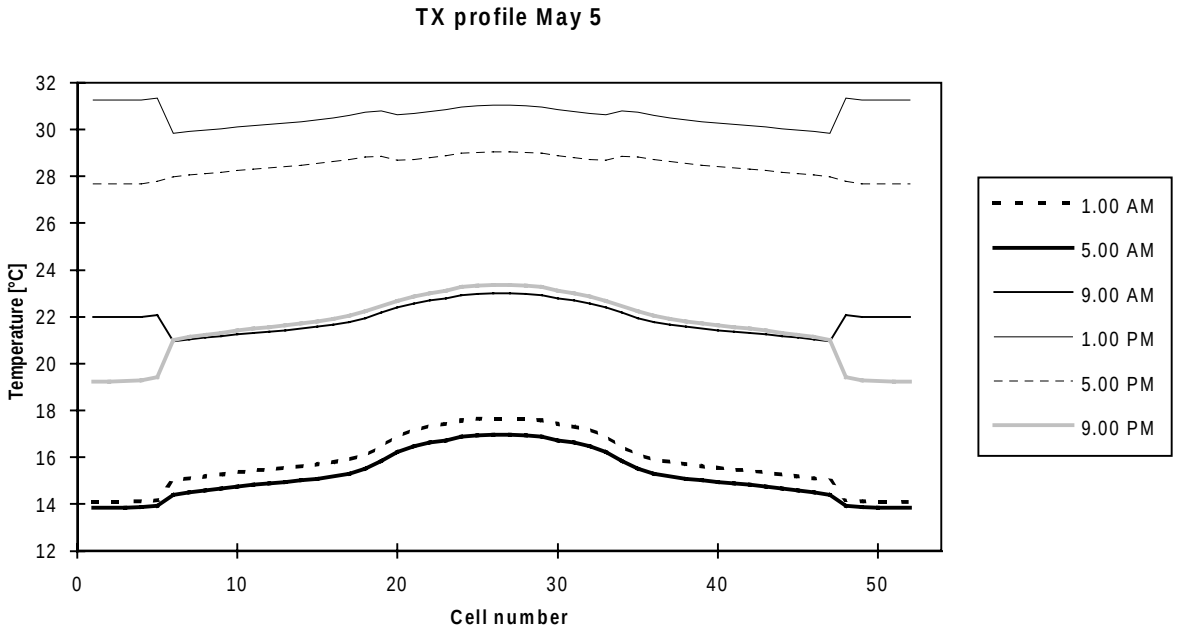

Figure 4.5 TX profile under nonuniform ground conditions.

Two facts can be determined which are of interest for practical applications. At first, some temperature distributions during the day exhibit a " wing profile " similar to that observed also in experiments in Studsvik (see Figure 5.3 a and 5.5). The primary reason for the observed wing profile was believed to be a heat resistance between sensors and ground surface. However, a similar tendency has also been observed with IR measurements during the daytime, see Figure 4.6.

The dip in the wing occurs during daytime with the solar irradiation heating the ground and raising the temperature level. The location of the dip is at the transition between sand bed and surrounding ground, i.e. from lower thermal conductivity and heat capacity C in the sand bed toward higher values in the surrounding soil. Another transition takes place at the edge of the asphalt layer at a distance of 6 m from the center line. Because of the large size of the node width in this point (1 m), the transient appears quite abrupt, which is of course an artefact. However both heat capacity and thermal conductivity decrease in the transition from asphalt to the surroundings.

Figure 4.6 shows the profile measured by the IR camera at an instance where the wing profile was distinct. This event occurred at noon of July 8 at the Studsvik test site. It is obvious that the thermal diffusivity of the upper layer plays an important role in determining the shape of the TX profile. A wing profile could be explained by the fact that the impressed heat flow from the pipes causes the soil near the pipes and all the way up along the centerline to be more dry than the outer parts of the

soil. This in turn causes the conductivity and the heat capacity to change slightly within the integration zone and thus the TX profile may also be affected. However, this does not necessarily mean that the TX factor is also affected under all conditions, as it is further explained by examining Figure 4.7.

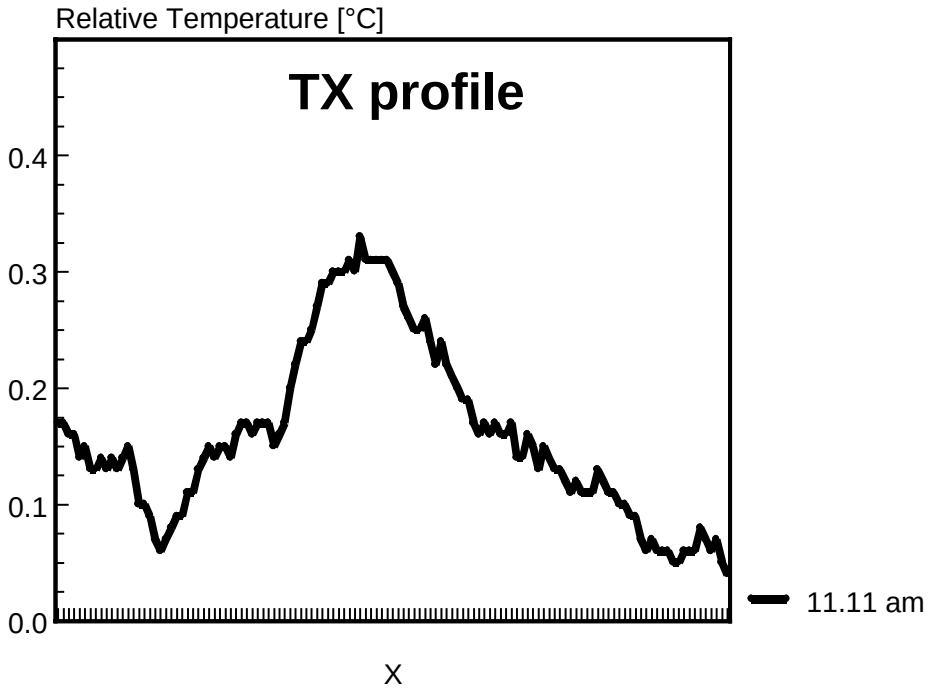

Figure 4.6: TX profile with expressed wings from test field in Studsvik at a very sunny day, July 8, in Studsvik. surface temperature T and width X in relative units (total width = 4.5 m).

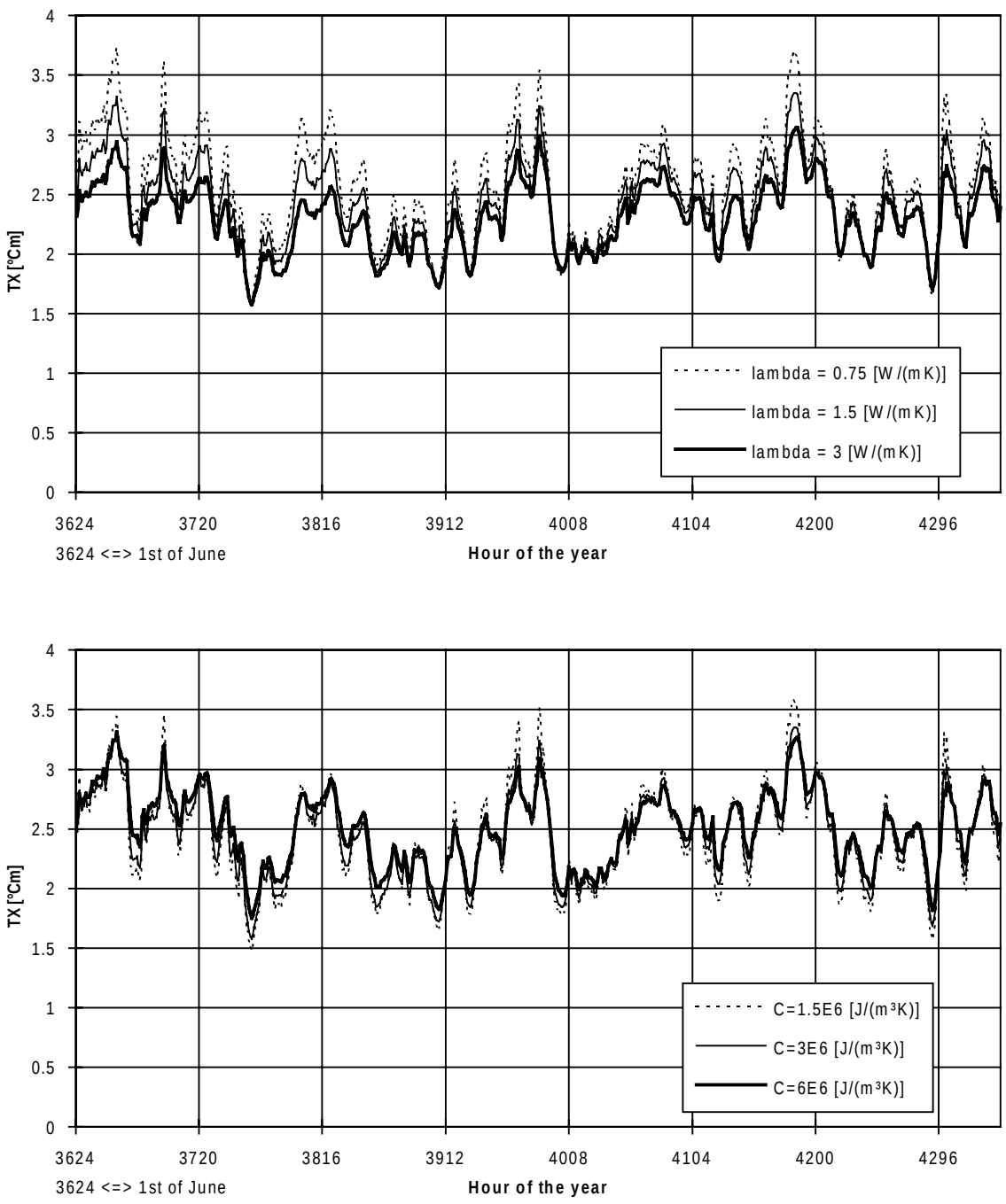

Figure 4.7 : Variation of the TX factor in time for different values of λ and C in the ground. Stockholm 1986.

Figure 4.7 shows the variation of the TX factor during a couple of days from simulation with the Stockholm 1986 climate. Different soil conditions have been investigated according to the table and the sketch inserted in the Figure 4.7. The values of thermal conductivity and heat capacity, and hence of the thermal diffusivity, might affect the amplitude of the TX factor fluctuations. Therefore these parameters may have a significant impact on the hysteresis effects and thus the instantaneous measurement of the TX factor. The resulting time constant is inverse proportional to the heat diffusivity *a*. A larger value of the diffusivity will increase the fluctuations and vice versa. However the mean value of the TX factor is only very weakly affected by both the thermal conductivity and the heat capacity as it will be further shown in section 4.3.

Figure 4.7 shows the variation of the TX factor during a couple of days from simulation with the Stockholm 1986 climate. Different soil conditions have been investigated according to the table and the sketch inserted in the Figure 4.7. The values of thermal conductivity and heat capacity, and hence of the thermal diffusivity, might affect the amplitude of the TX factor fluctuations. Therefore these parameters may have a significant impact on the hysteresis effects and thus the instantaneous measurement of the TX factor. The resulting time constant is inverse proportional to the heat diffusivity *a*. A larger value of the diffusivity will increase the fluctuations and vice versa. However the mean value of the TX factor is only very weakly affected by both the thermal conductivity and the heat capacity as it will be further shown in section 4.3.

4.3 THE INFLUENCE OF DIFFERENT PHYSICAL PARAMETERS ON THE TX FACTOR

4.3.1 The phase shift between surface temperature and TX

As mentioned in the previous section, the thermal conductivity of the ground and the heat capacity of the ground will affect the instantaneous TX factor by introducing a time constant to the heat flow. The result of that will be that any change in the energy balance, due to wind, a change of the ground temperature, or of the surface temperature will take some time to be expressed in a corresponding temperature profile and hence TX value. Thus, the instantaneous TX factor might fluctuate as shown in Figure 4.7.

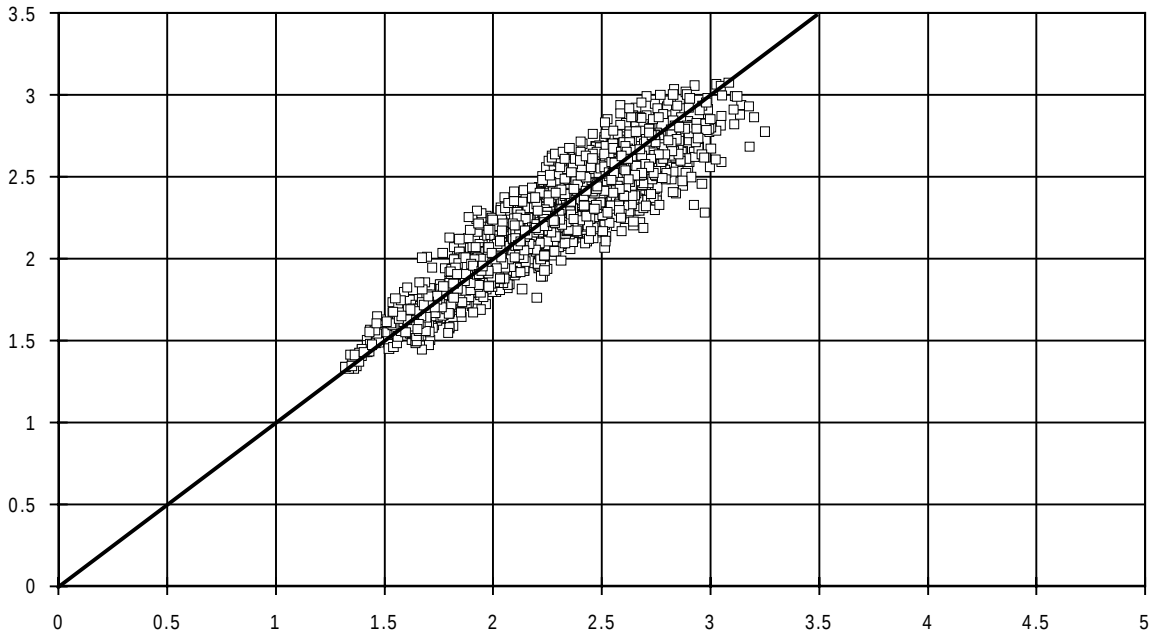

Figure 4.8 Correlation of the TX factor for Stockholm 1986 and its mirror climate, resulting in a phase shift of 6 hours.

To find this time delay, we constructed a synthetic climate by "reflecting" a climate file for three months making it symmetric around a certain day. Thus the resulting climate for the next three months is essentially the same as for the preceding three months but in an inverse time direction. The correlation between the hourly values of TX for the first three months and for the reflected three months shifted by 7 hours, thus indicating a phase shift of the TX factor by three hours, as it can be seen from Figure 4.8.

Similar conclusions can be drawn from the hourly plots around the mirror point at the right boundary of the diagram shown in Figure 4.9. The fluctuations are shifted by 6 - 7 hours, indicating a response time of about three hours on each signal.

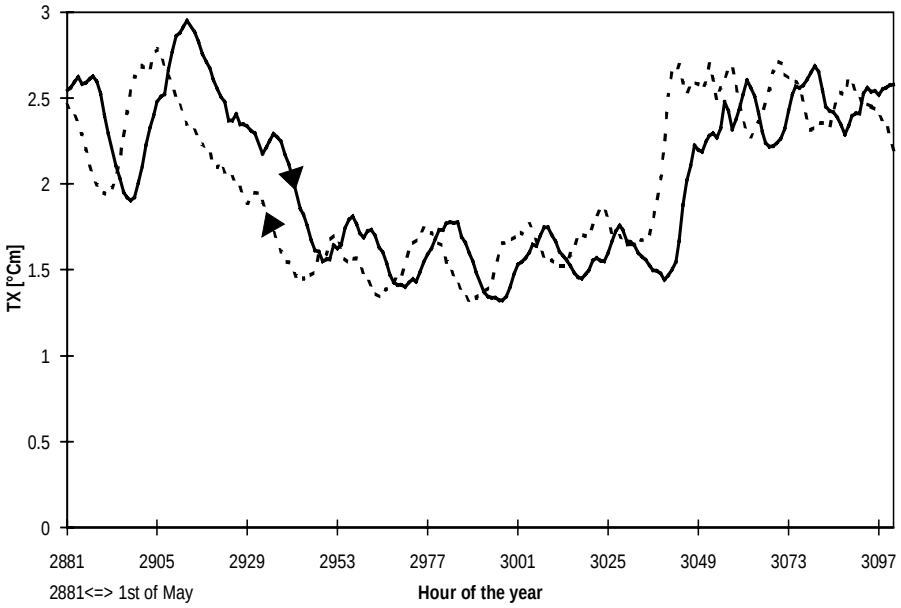

Figure 4.9 Phase shift between Climate and mirror climate, Stockholm 1986.

Equation (7) tells us that for this response time of the TX factor approximately the upper 3 cm of the soil are involved in the rapid fluctuations of the TX factor.

One of the parameters contributing to these fluctuations is the changing surface temperature. The surface temperature varies due to changes in the ambient temperature and the solar radiation. Its influence is relatively weak at stronger winds but relevant for winds below 1 m/s. This can be seen from Figure 4.10 showing the daily variation of TX and of the surface temperature for two otherwise identical hot summer days, one with and the other without wind.

The best regression fits for interpretation models were achieved by taking into account the temperature changes on the surface during the last hours before the measurement time. A suitable correction was found by means of regression analysis by defining a quotient of the average temperatures during the last 14 and 24 hours respectively: $\Phi_T = \langle T_s 14 \rangle / \langle T_s 24 \rangle$ (see also Chapter 6). The reason for using averages rather than instantaneous values for both surface temperature and wind (see also Chapter. 4.3.3) is to introduce a filter for the short abrupt variations and in that way address the inertia of the upper ground layer. At higher wind speeds, its influence becomes dominant. The influence of the changing surface temperature on the TX factor can no longer be seen in the multiple linear regression fits at wind velocities larger than 1 m/s. For such wind conditions, the fluctuations and the time phase shift increases slightly, as shown in Chapter 4.3.3.

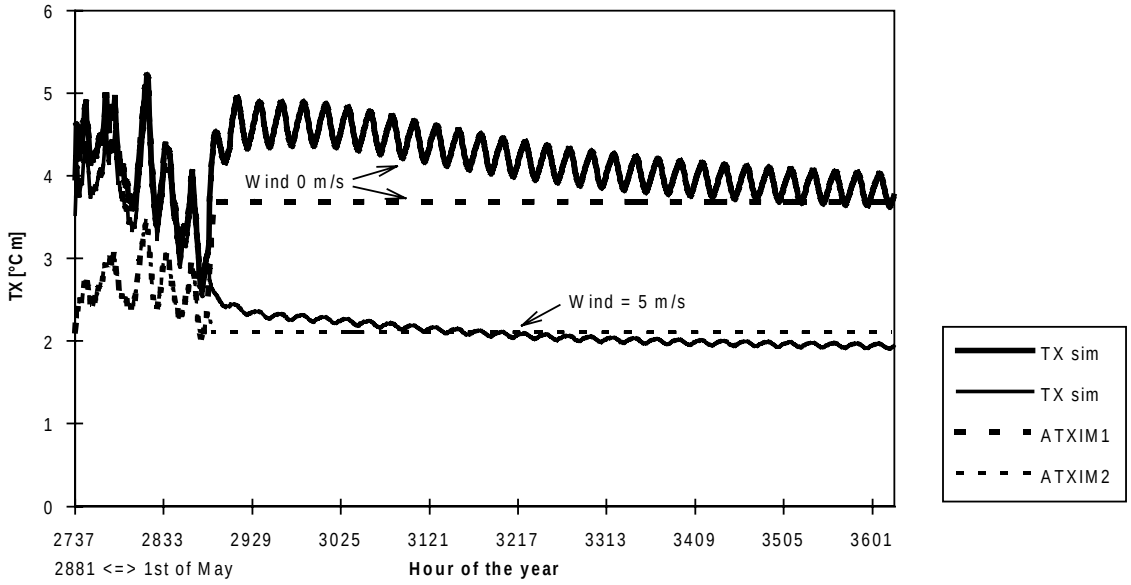

Figure 4.10 Variation of the TX factor and surface temperature for no wind and strong wind respectively for the same conditions of the heat loss of the pipes.

4.3.2 Heat conductivity and heat capacity

The earlier discussion of Figure 4.7 makes it clear that the heat diffusivity $a = \lambda / C$ will affect the instantaneous measurement of TX. A variation of C and λ values by a factor of two indicates that there will be a change in the amplitude of the TX factor resulting in an uncertainty of 10% in the absolute value of TX factor. However, because the fluctuations are around a mean value, the error could be either positive or negative, and it is therefore not easy to include this effect in an analysis for a single measurement.

It is, however, easier to make conclusions about the influence on the mean TX value. Annual simulations were made with the heat capacity C being varied between 1.5 and 6 MJ/(m³·K) and the thermal conductivity between 0.5 and 3 W/(m·K). The result is shown in Figure 4.11: The mean value of the TX factor based on averages for the summer shows only a minor dependence on C and λ.

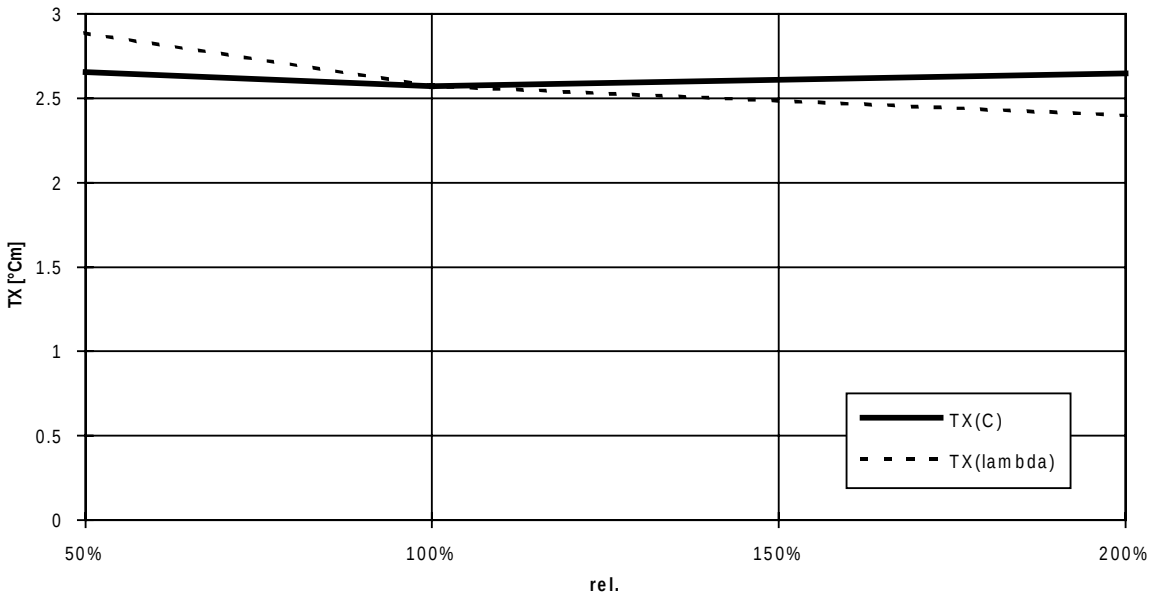

Figure 4. 11 The mean value of the TX factor as a function of (uniform) heat capacity and thermal conductivity of the soil. 100 % corresponds to λ = 1.5 W/(m·K) and C = 3.0 MJ/(m³·K).

4.3.3 Wind

The heat loss from the surface is partly caused by convection heat transfer to the air. Convection can be of two kinds, natural and forced. Forced convection due to wind is the dominant mode here. A problem arises from the way the wind speed is normally measured. According to meteorological standards wind speed is measured on masts at a height of 5 m above ground. Usually, at this height, the wind speed is much higher than close to the ground surface. The equations used for the calculations of the convective heat loss from the ground are based on this standard measurement techniques and should therefore be applicable on open surfaces. However, in many situations the ground might be sheltered and hence the influence of the wind, which is to flatten the temperature profile, could be overestimated. This in turn would result in a overcorrection of the TX factor due to the assumed higher wind speed and ultimately the higher TX factor would result in a higher estimate of heat loss.

The influence of the wind on temperature profiles were measured by Jönsson, Zinko (1992), see Figure 4.12. From this figure the flattening of the TX profile with increasing wind due to forced convection can be clearly seen.

From these experiments it became obvious that the wind speed is a very important parameter, **probably the most important single parameter,** affecting the TX factor. Figure 4.13 shows measurement values of the TX factor and wind speed for an transition from low to high winds.

Figure 4.12 Temperature profiles when the surface is exposed to wind.

Figure 4.13 Wind influence on the TX factor as measured at the test field in Studsvik.

It can be seen that the TX factor is drastically reduced by the wind, from about 5 to 2.5 when the wind increased from 0 to 5 m/s on a day in October. A simulation for similar conditions gives quite similar results as indicated in Fig. 4.13 by the dashed line. It can also be seen from this figure that the time constant for the transition is about 10 hours. In Studsvik and in many places near the coast, it is blowing quite often. **Hence it is to expect that the wind has a pertinent but stochastic influence on the TX factor and is responsible for the strong fluctuations of TX** as it can be seen from the Figures 4.1 and 4.2.

A regression analysis made for Studsvik that was based on the 1986 summer period in Stockholm using zero, first, and second order in wind speed gave no conclusive result. However, from step functions similar to those of Figure 4.13, we derived a function for the long term average dependence of the TX factor on the wind velocity. The influence was assumed to be as shown in Figure 4.14, following a negative e- function. We assumed that the basic relationship was of the form $TX \sim A + Be^{-Cw}$ and then used linear regression based on hourly values to yield the following important result:

$$TX = 1.34 + 2.35 \cdot (0.8)^{<w7>} \qquad (11)$$

The parameter <w7> signifies that the average wind speed of the last 7 hours should be taken for the calculation of TX. This average takes care of the phase shift due to the thermal inertia of the ground.

The relationship according to Equ.(11) is shown in Figure 4.14 compared with the actual fluctuations of Stockholm 1986 weather data.

As it can be seen from the comparison of the interpretation model with the annual simulation for Stockholm weather for 1986, a reasonable agreement between interpretation model and simulation model can be achieved by introducing the wind according to Equ.(11).

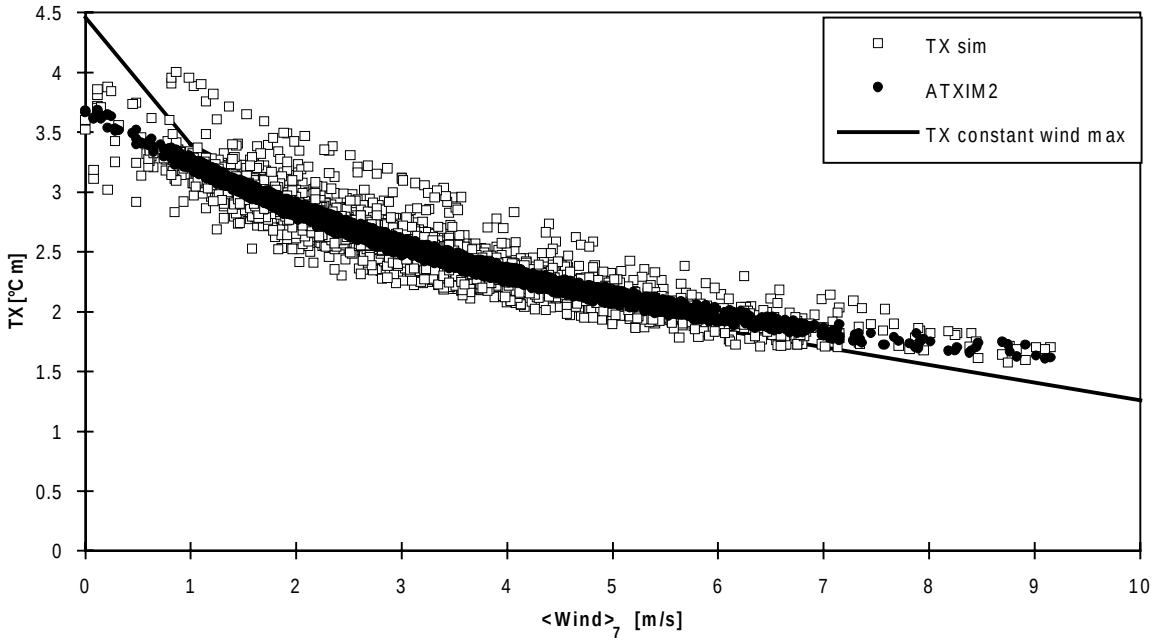

Figure 4.14 The wind model in comparison with hourly results from simulations for Stockholm 1986. ATXIM2 refers to equation (16).

4.3.4 Precipitation

The experience with wet surfaces is not very conclusive. In Jönsson, Zinko (1992), it could be shown that the evaporating process on drying surfaces cools the surface, the stronger, the higher the temperature of the surface. Hence the temperature profile is flattened out, resulting in large TX factor transients as indicated in Figure 4.15.

Figure 4. 15 Measurements of the TX factor at Studsvik's test field with dry and wet surfaces.

It can be seen from Figure 4.15 that wet surfaces can still exhibit a TX factor, but smaller compared to dry surfaces. A further example can be seen from Figure 4.16, showing a TX profile taken in Lyngby, Denmark, in November 1995.

A theoretical model of treating precipitation must include the thickness of the water layer on the surface and of the water content in the ground. Principally it is no problem to treat these parameters in the simulation program. The problem is to get relevant input data from field measurements and to decide if the wet state is steady or transient. Simple measurement techniques for the purpose of thermography must then be developed or refined. Hence, our judgement is that the situation of including precipitation on the quantitative evaluation of heat losses cannot be handled in an unambiguous way. Most experienced thermographers will avoid making thermographic measurements on wet surfaces. **Therefore we decided to refrain from attempting to apply the TX model under conditions of rain and/or wet surfaces.**

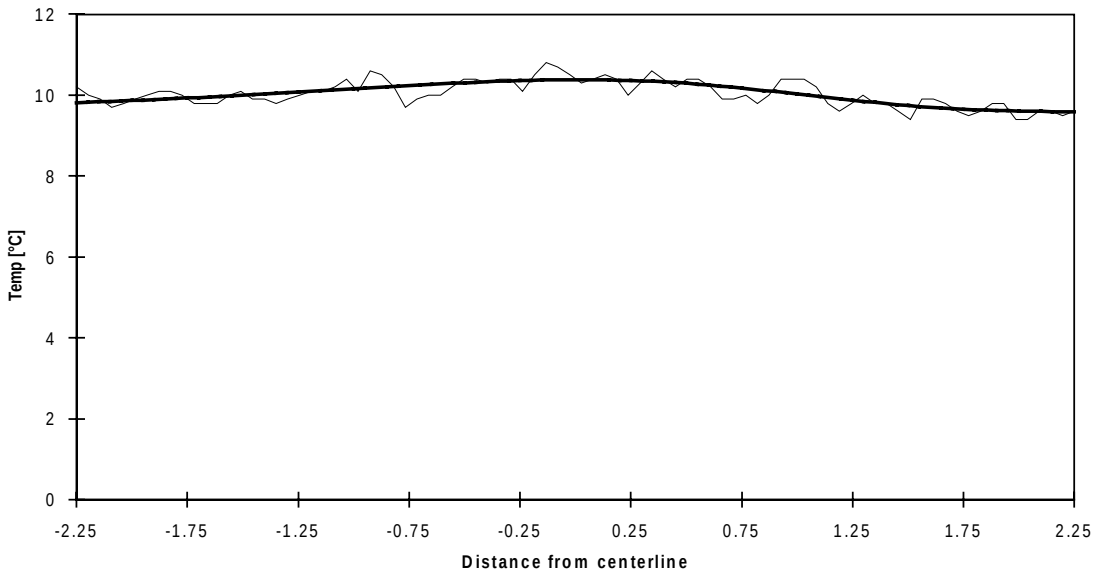

Figure 4.16 The TX factor from a rainy day in at the test-site of Karlstrup, Denmark. The thin line shows the measured IR profile, thick line is the smoothed profile used for TX evaluation.

4.3.5 Change of district heating pipe temperature

Of course a very important physical behaviour is the response of the TX factor to any change in the temperature of the district heating pipes. This change can come from changing the distribution temperature (supply and/or return) of the water in the pipes or from an occurring damage in the pipe insulation. This situation was extensively treated in Jönsson, Zinko (1992) and is summarised in this chapter.

In order to verify the models for dynamic effects, we have performed simulations with an instant change in the heat loss from the pipes and studied the subsequent changes in the TX factor for the following days. This case assuming that an instantaneous damage to the insulation takes place will rarely occur in reality. It is, however, a meaningful case to investigate the dynamic response at the ground surface. The calculations have been verified with measurements at Studsvik's test field by instantaneously increasing the heat loss from 55 to 95 W/m. The influence of the damaged pipe on the surface temperature has then been studied.

If the aim is to quantify the heat loss by thermography, the relation between the TX factor and the real heat loss is of importance. It was found that the quotient formed by dividing the heat loss in W/m by TX in K·m, is about 20 W/(m²·K). Figure 4.17 shows that any change in the pipe surface temperature results in a transient of this quotient which then is relaxing toward the initial value in a couple of days. That means that the signal of the heat loss under our conditions is stabilized 5 - 10 days after the change in the surface temperature of the pipe.

The peak in the heat loss at the occasion of the damage is due to absorption of sensible heat in the soil close to the pipe during the transition time. Figure 4.17 shows that the relation between the heat loss and the TX factor can be as much as three times during the transition. Thus the TX factor cannot be used to quantify the heat losses in the first week after a damage has occurred.

Figure 4.17 Heat loss divided by TX factor at the days around the heat loss has been increased in a pipe. Simulation Stockholm 1986.

This is also confirmed by field measurements, see Figure 4.18. In May 1991 the electrical power was increased to simulate a damaged pipe. The power supplied was increased from about 55 W/m to about 110 W/m. Figure 4.18 shows the effect of the increase of the heat loss on the TX factor on 7 May 1991. After about 5 days the TX factor approached the new value.

The most important conclusions to be drawn from these observations is that the measured TX factor will reflect the status of pipes as it was 1 - 2 weeks before the measurement.

4.3.6 The buried depth of pipes

It has been shown in Jönsson, Zinko (1992) that the depth of the pipes in the ground is a very important parameter for the value of the TX factor and hence for the determination of the heat loss using this method. The depth must be known accurately, and if this is not the case, it should be measured by some suitable commercially available instrument.

Figure 4.18 Change of heat loss in the test field in Studsvik: Response of TX factor.

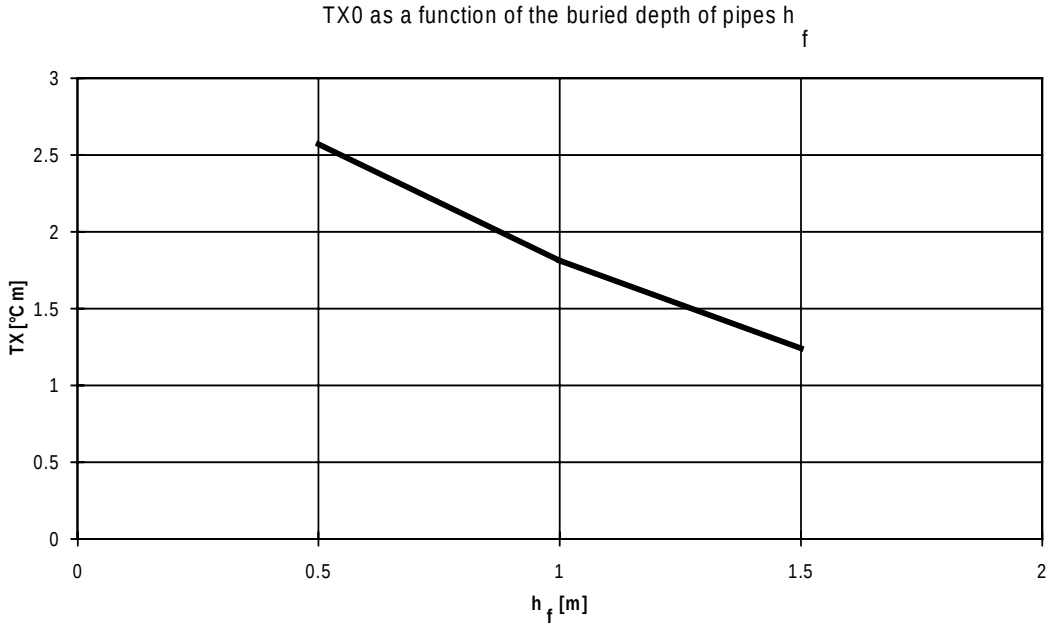

Figure 4.19 TX0 as a function of the buried depth of pipes h_f.
By carrying out simulations with different depth of the pipes, a relationship between the long term average of TX for the reference case, TX0, and the buried depth of pipes, h_f, could be established, as shown in Figure 4.19.

4.3.7 Integration width

The width of the TX profile is depending on many parameters, among them depth of pipes, wind speed and thermal conductivity of the ground. Figure 4.20 shows TX as function of the integration width based on IR measurements from Studsvik. The TX factor increases with the integration width 2X (X measured from the centerline). The measured IR profile approaches an inflection point toward an asymptotic value. In the test field in Studsvik, this point was reached at an integration width 2X of 4.5 m. It is recommended to use this integration width in field measurements. ATXIM gives an approximated function for that valid for 2 X = 3.5 to 5 m.

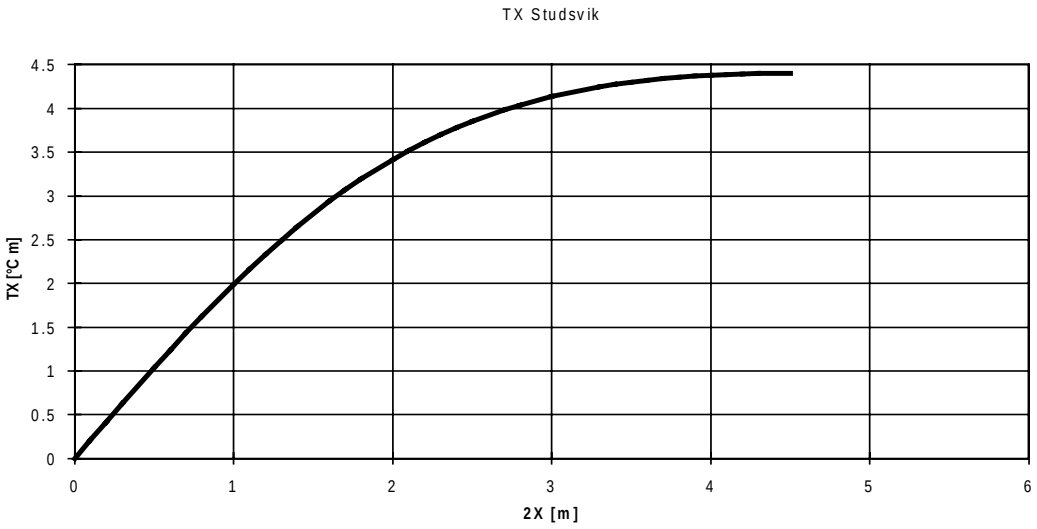

Figure 4.20 TX factor as function of the integration width 2X.

5 TX - measurements on test fields

5.1 EXPERIMENTS IN STUDSVIK, SWEDEN

5.1.1 The Test field

The experimental set-up of the test field in Studsvik is described in detail by Jönsson, Zinko (1992). The field comprises an area covered by asphalt, 9 m x 12 m with a centrally placed two-pipe system underneath. The pipes, 9 m long and 200 mm in diameter are placed 0.5 m below the surface in a sand bed according to the practice for pre insulated jacket pipes (see Figure 5.1). The pipes were electrically heated and the normal operation was at constant power of 500 W supplied all year round by means of electrical pipe heating wires mounted on both pipes. This resulted in a total heat loss from the pipes surface to the surroundings of 55 W/m. The test field was operated in the years 1987 - 1991, and for the use in these investigations, from April 1994 to the end of 1995.

Figure 5.1 Cross section of the test field with location of sensors.

The main purpose for the experiments in Studsvik was to collect long-term data for the TX-factor. For this purpose, the surface temperature was measured by means of Pt-100 temperature sensors glued to the asphalt in the middle of the field and perpendicular to the direction of the pipes. The outermost sensor was placed 4.48 m on each side of the pipe axis. These sensors served as a reference temperature for the undisturbed ground. The nine innermost Pt-100 sensors were placed with a pitch of 0.56 m. Two heat flow meters were also installed, one on the pipe axis and the other

one in 4.48 m away from the axis. The pipe surface temperatures and the temperatures at 1 m below the pipes and 0.3 m above the pipes were also measured.

A data logger system (HP-86) monitored temperatures, heat flows, supplied electrical power as well as climate data including solar radiation, net infrared radiation, air temperature, wind velocity and rain indication. The sampling time was 2 minutes. These values were averaged to hourly means and stored for off-line evaluation. The TX-factor based on X = 4.48 m was also calculated, averaged and stored.

5.1.2 Measurements with Pt-100 sensors

Results from the measurements with Pt-100 sensors for May 1990 are shown in Figure 5.2. It can be seen that the TX-value showed strong fluctuation with a periodicity of 1 day during a period with sunny weather in May 1990.

Figure 5.2 Sample of TX values recorded by means of Pt-100 sensors in May 1990.

However a more detailed analysis showed that one could discern the behaviour of the TX fluctuations at sunny hours from that of night time and cloudy conditions. Figure 5.3 a - d shows an example for the variation of the TX-profiles of a clear day and night as well as under cloudy conditions.

The corresponding TX values for the normal reference conditions of a heat loss of 55 W/m are depicted in Figure. 5.4 a, b.

The fluctuations of the TX factor are strongly enhanced by sunshine conditions but relatively small with low or no incident solar radiation. The reason for that became clear much later when we performed measurements with a rubber sheet covering the asphalt surface including the Pt-100 sensors: When the sun is shining, even a small heat resistance between the Pt-100 sensor and the ground surface will let the sensors appear to be hotter compared to the true surface temperature. The sensor will appear

cooler at night, when the heat flux from the black painted sensor is reversed through radiation. Different resistances at the individual sensors can bias the resulting TX-factor, resulting in the apparent strong fluctuations. This effect has not been seen in earlier years and must be a result of the ageing of the glue used.

a)

b)

c)

Figure 5.3 a - c TX-profile: a) sunny day; b) clear night; c) cloudy day.

Figure 5.3 d TX-profile: d) cloudy night.

a)

b)

Figure 5.4 a - b TX factors measured with Pt-100 sensors on a sunny and on a cloudy day, respectively.

This effect will be avoided by IR measurements. *As we will see in the section 5.1.4, sunny conditions can also be used for the determination of the TX-factor by using suitable IR equipment for the determination of the TX factor instead of the measurement of the surface temperature with sensors.*

5.1.3 Measurements with rubber cover

A principal problem with quantitative thermography is the emissivity of the surface and its uniformity over the integration widths. Therefore different ideas were discussed for using reference surfaces as cover. In the US investigations, asphalt shingles as cover on grass and soil surfaces were successfully tested (see section 5.4). In Studsvik, we investigated a rubber sheet as a reference cover on the ground surface.

Figure 5.5 TX profile from Pt-100 sensors covered with rubber sheets laid on the asphalt surface.

Figure 5.5 shows a result from these measurements. The results were deemed unsuccessful and therefore testing was abandoned after a while. The test surface was covered with two black rubber sheets with high emissivity ($\varepsilon = 0.9$), 2 m in width and 2 mm thick. The sheet covered also the temperature sensors. However because of the large surfaces ($2m \times 6m$) of each of the sheets, it was very difficult to get a good contact between the asphalt and the rubber. Instead the rubber cover served as an extra insulator of the surface with a small air gap between rubber and asphalt. The result of that was an accumulation of heat above the pipes and quite a linear decrease in temperature from the centreline towards the outside edges. On the other hand, when the sun was shining, the rubber sheet acted similar to a solar collector with the temperature profile flattening out. Whereas the TX factor during the night

reached values between 10 and 15, the TX factor during sunny conditions was only between 1 and 2.

Hence a reliable procedure for evaluation of heat losses could not be established with this type of rubber as a reference cover.

5.1.4 IR-measurements

The largest drawback in this project was the lack of modern IR-Thermography equipment for continuous use. We are therefore very grateful to AGEMA, Sweden, for providing us with a modern IR thermography camera of type AGEMA Thermovision 470 Pro in summer 1995 for measurements at the Studsvik test-site. Although this camera operates in the near IR and thus the daylight results could have been disturbed by the solar radiation, the sun filter of the camera worked very well. This allowed us to work during daytime for quantitative determination of TX factor and heat losses.

The camera AGEMA Thermovision 470 Pro is battery driven, microprocessor controlled, and electronically cooled. It can be operated in both the temperature profile mode and the isotherm mode. The pictures are stored electronically on discs for PC supported analysis later on (The PC analysis can also be done on-line, but we did not use this option).

A menu on the screen helps to set all the necessary parameters for physical camera adjustments (such as sky and ambient temperature, emission coefficients, distance to the object), for mode selection (isotherms, profiles, spots), temperature range settings and disc storage control.

In general there are three types of camera lens systems available for different sight angles. However, in our case we had only the lens system with an aperture angle of 20° at our disposal. In order to investigate the TX profile along a 4.5 m long line, the sensing distance must be about 12 m. A sky lift was used to reach a necessary height of 6 m. Hence the sight angle to the middle of the test field was about 30° (see Figure 5.6).

The purpose of our measurements was to make a quasi continuos evaluation of the TX profile as to be measured by IR equipment and compare it with Pt-100 measurements. Hence we investigated the TX profile over a period of 40 hours during the period of 7 - 9 July 1995 by taking IR-images from the sky-lift at intervals of about 20 minutes. The images were stored on a disc and evaluated later in the office by means of the evaluation program IRwin 2.0 supplied by AGEMA.

The following ***evaluation procedure*** was observed:

The discs were read into the program and automatically adjusted to show the thermograph of the field with the optimal thermal resolution. In the picture, the integration boundaries can be positioned according to the marking points for the 4.5 m

line as shown in Figure 5.8. The line profile can then be plotted directly from the picture (Figure 5.8 b, d). These Figures show an example for the day and for the night, as well the IR image as the TX profile.

Figure 5.6 View from the sky-lift over the test-site showing the marking for the line along which the TX profile is taken.

Figure 5.7 Sky-lift arrangement for making TX diagnosis with IR camera.

a) d)

b) e)

c) f)

Figure 5.8 a-f Infrared pictures and TX plots for day (a, b, c) and night (d, e, f).
The next step is the evaluation of the TX-factor. This could be done most efficiently by writing a subroutine to IRwin. 2.0. However, because the program code was not available to us we made the TX integration in EXCEL with which IRwin 2.0 easily can communicate. However, before making the integration we applied a profile smoothing procedure as shown in the images c and f. This is necessary because the integration procedure is looking to the local minimum on both outside edges of the profile. A local minimum caused by noise would result in too large a TX area, as indicated by the broken lines in Figure 5.8 c and 5.8 f, respectively.

This procedure was applied on about 120 images taken at Studsvik. The measurement period fell in the beginning of a very warm Swedish summer following a period of rainy weather, initially somewhat cloudy on the afternoon of the July 7th, but clear and nice the remaining period with short summer nights. The wind was close to zero except for a few hours during the afternoon of July 8th, when a local sea breeze caused some clouds to move over the area.

Figure 5.9 shows the resulting TX factors taken by the IR camera together with some climate information for the entire measurement period (July 7th at 2 p.m. until July 9th at 5 a.m.)

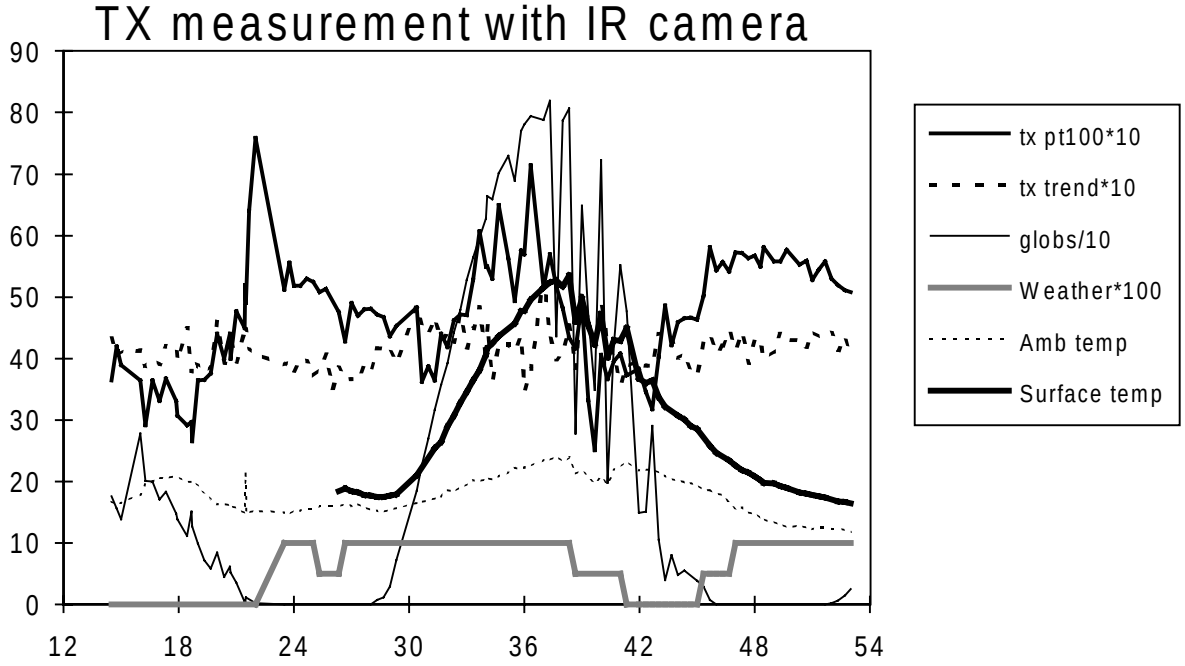

Figure 5.9 TX factors and climate information for the period of IR measurements in Studsvik. TX profiles are based on Pt 100 and IR (=TX trend) respectively. Solar radiation on horizontal surfaces (=globs). Weather: 10 clear, 5 = half clear, 0 = cloudy).

From Figure 5.9 it can be seen that the uncertainty of each individual image might be relatively large. The TX factor varies between 3.6 and 4.9, i.e. ± 15% in this measurement series. As can be expected, the noise is getting larger during day time and smaller in the night. The measurement error acts like a noise signal added to the true signal. To further analyze this, we applied an attenuation to the signal by converting it to a moving 5 hour average. These signals can then be compared with signals from the Pt-100 sensors. As shown in Figure 5.10, referring to the description in Ch. 5.2, the results are not surprising: The TX factor based on IR measurements varies weekly during the measurement period, whereas the TX factor based on Pt-100 sensors exhibits very strong fluctuations. However the night values agree quite reasonably, within 10 % for both methods. In Figure 5.10, the measurements are also compared with simulation results for the TX factor and with the calculated value of TX according to ATXIM (equations (15) and (16)) with known pipe heat losses. Unfortunately, experimental infrared radiation data were lacking from this measurement period. Therefore the agreement between simulation and experiment is not too good, but the averages values are of the right magnitude.

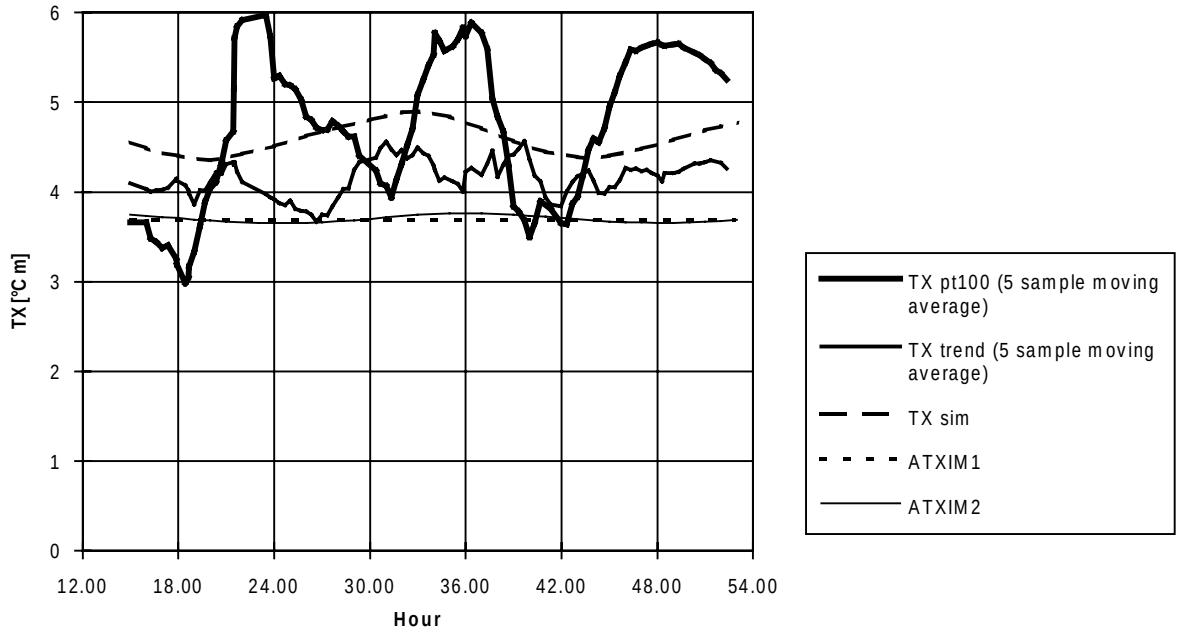

Figure 5.10 A 5 hour mean average of the TX factor measured by IR compared with the TX factors of the Pt-100 sensors. TXsim = result from the simulation with estimated IR and wind values. TXtrend = IR average over 5 samples. ATXIM 1 and 2 refer to equations 15 and 16 respectively.

The Pt-100 measurements fluctuate very strongly and are considered not to be reliable during the sunny daytime. The IR measurements, here called trend5 because of the integration over 5 consecutive samplings, are relatively constant all the time.

Thus as a result from these measurements we can state that the evaluation of the TX factor by means of the IR equipment is a straight forward method as long suitable conditions (homogenous surface, no shading, no rain) exist. Especially interesting is that the method can be used also at sunny days.

What remains to investigate is a method for determining the heat loss based on TX factors directly measured with an infrared camera. This procedure is described in Chapter 6.

5.2 EXPERIMENTS IN LYNGBY, DENMARK

5.2.1 The experimental site and set-up at the Technical University of Denmark (TUD)

The experimental site and set-up were chosen very carefully. A grass-covered area in the north-west corner of TUD was found very suitable, because this area had previously only been used for farming. From a nearby geotechnical drilling it was expected that the soil would be rather well-sorted moraine sand.

Furthermore the distance to nearby buildings and sewer and water pipes was so large that no influence on the temperature field in the ground was expected. A few tall trees would not cause serious problems by making shadows.

As the public had access to the area serious consideration had to be given to protection of the experimental set-up.

The experimental set-up is shown in Figure 5.11. The experimental pipe was an uninsulated 273 mm steel pipe, 12.35 m long, including the buried pump and heater unit. A small expansion tank was placed inside the experimental pipe.

This design was chosen because one isothermal (steel) pipe theoretically has a more well-defined thermal resistance in the soil than two non-isothermal (polyethylene) pipes as normally used in DH systems. Furthermore the symmetry of the one-pipe system could be utilised in the instrumentation of the system.

Figure 5.11 The experimental set-up in Lyngby.
The experimental pipe was guarded by two 6 m long 273 mm steel pipes, one in each end of the experimental pipe. The pump, heater and expansion tank for these pipes were hidden in a buried ventilation duct. Styropor insulation 3 m² of 4 cm thickness was placed between the guard pipe and the ventilation duct to further protect the temperature field in the ground. Styropor insulation disks 2 cm thick (with diameter 273 mm) were placed between the experimental pipe and the guard pipes.

The pipes were installed in a narrow trench 0.9 m deep and the soil (moraine sand) was backfilled into the trench just after instrumentation had been completed. The depth of the pipes was approx. 0.75 m.

The pipes were heated by circulating water from the heater through a 168 mm concentric pipe inside the 273 mm pipe and back to the heater.

The control strategy was to keep the water temperature constant so that a steady state would exist between the supplied amount of heat and the heat loss from the pipe.

In a real DH pipe system the temperature of the casing will vary with the temperature in the soil. The experimental set-up at DTU exaggerates the seasonal variations by maintaining a constant casing (water) temperature while the experimental set-up at Studsvik disregards the seasonal variations by applying a constant heat input to the pipes.

From October 1992 to July 1994 a constant water temperature of 25°C was used. Because of the very hot summer in 1994 the heat from the pump caused the pipe temperature to rise, see Figure 5.12. On 6 August 1994 the setpoint was raised to 35°C. A major rain storm disturbed the control on 15 September 1994. On 1 October 1994 the experimental pipe was allowed to cool to 17.5°C. In January 1995 the setpoint was finally changed to 10°C.

Figure 5.12 Pipe temperature from January 1994 to March 1995.
By the end of 1993 an area of 4 m × 7 m was constructed of 8 cm thick concrete tiles for making infrared measurements of the heat loss, see Figure 5.11.

In August 1994 two 2 m long pipes were buried South of the instrumentation container. One pipe was an uninsulated 273 mm steel pipe and the other was a preinsulated 60 mm pipe with casing diameter 125 mm. These pipes were heated directly by electricity and the main purpose was to investigate calibration errors of heat flux meters.

5.2.2 Instrumentation

The pipe temperatures were controlled by seven thermistors T1-T7, see Figure 5.11. At the middle of the experimental pipe (T1) additional temperature sensors were installed, i.e. one Pt 100 sensor and one thermocouple. These sensors were placed in pockets in the steel pipe which were filled with copper grease.

The temperature differences between the guard pipes and the experimental pipe (T2-T3, T5-T6) were also measured by 5 differential thermocouples in series, which were actually used for the control.

On a PVC frame at the middle of the experimental pipe 28 differential thermocouples and 28 thermistors were placed, see Figure 5.13. The reference junctions of these thermocouples were placed in the same pocket as previously mentioned so that the absolute temperatures could be obtained from temperature T1.

To measure the heat flux distribution 8 heat flux meters (HFM) were installed at location T1. For control purposes additional HFMs were installed at locations T2, T3, T5 and T6, see Figure 5.14. The HFMs were fixed to the pipe surface by epoxy. Plate HFM with dimensions of 15×80×2 mm from International Thermal Instrument Company, type 150, were used (λ = 0.8 W/(m·K)).

Figure 5.13 Differential thermocouples and thermistors on a PVC frame.

Figure 5.14 Locations of the heat flux meters.

Undisturbed soil temperatures were measured in two locations, one perpendicular to the middle of the experimental pipe, and one East of the instrumentation container. At each location the temperature was measured in seven heights with both thermistors and differential thermocouples. The reference junctions were collected in an isothermal tube. The temperature of this tube was measured with both one thermocouple, one thermistor, and one Pt 100 sensor.

The heat flux at a depth of 0.1 m was measured in both locations. In the middle (undisturbed) the heat flux was also measured at a depth of 0.275 m. Plate HFM with dimensions 100×100×2 mm from International Thermal Instrument Company, USA, were used (λ = 0.8 W/(m·K)).

The surface temperature distribution of the concrete surface was measured both with thermistors and with differential thermocouples made of five thermocouples in series, see Figure 5.15. The absolute surface temperature was measured with a single thermocouple connected to the electrical ice point inside the instrumentation container. The sensors were cast in concrete in spaces between the concrete tiles, and placed close to the surface, i.e. covered with 1 - 2 mm of concrete.

At the top of the instrumentation container the air temperature was measured. Also, from February 1994, incident solar radiation, wind speed and wind direction were measured at the top of the container.

In addition to these measurements weather data have been collected at the Thermal Insulation Laboratory, TUD, located approx. 100 m from the experimental site.

Figure 5.15 Locations of the surface temperature meters.

Different Hewlett Packard datalogging systems have been used to collect data. From the start of the measurements in October 1992 two HP 3497 systems were used. In March 1993 a HP 3852 with 140 channels was used instead because better resistance measurements could be made with this datalogger. This system had a built-in reference temperature junction for thermocouple measurements which was used to check the electrical ice point being used for absolute temperature measurements.

In January 1994 it was necessary to use one of the HP 3497 dataloggers to collect data from the surface temperature measurements and some HFM on the experimental pipe and on the two 2 m long pipes. (This datalogger did not make any resistance measurements).

Normally, all channels were scanned every minute and two hour mean values were stored in a PC connected to the datalogger.

The HP 3852 datalogger was calibrated just before it was taken into use by Hewlett Packard (Danish Accreditation Scheme, DANAK, no. 195). It was then used to calibrate the other dataloggers.

The copper - constantan thermocouple wire and one Pt 100 - sensor were calibrated at the Danish Technological Institute, DANAK no. 200. The NTC thermistors were then calibrated with the above equipment.

The heat flux meters were calibrated at one-dimensional conditions at the Thermal Insulation Laboratory.

The total electricity consumption for the heater and the pump in each pipe was measured by electricity meters. For the experimental pipe the consumption of the heater was measured separately. The electricity meters were calibrated by Landis & Gyr Laboratory in Vejle.

The electricity meter used for the total consumption in the experimental pipe was supplied with an integration unit which was connected to the PC system so that the electricity consumption could be recorded.

In addition to the surface temperature measurements the temperature profile was recorded by several infrared cameras by the IEA working group in September 1994.

5.2.3 Results

Figure 5.16 shows the heat loss (W/m) from the experimental pipe based on the electricity consumption. The heat loss based on the HFMs at the middle of the experimental pipe is also shown. These HFMs confirm the variation in the electricity consumption but the absolute value of the HFMs should be corrected by in-situ calibration.

Figure 5.17 shows the absolute surface temperature at the concrete area for infrared measurements. (In January 1994 the thermocouple used for this measurement was destroyed by a mouse). The measured TX-factor based on the differential thermocouples measurements is shown in Figure 5.18. It appears that the TX factor can be negative in the summer time. The reason is that the field was operated at constant temperature of 25ºC during a period of hot summer where the average surface temperature could have been close to this value or even higher. Late in August, the temperature of the pipes were increased and the TX factor became positive again.

Figure 5.16 The heat loss based on electricity consumption.

Figure 5.17 Absolute surface temperature of concrete surface.

Figure 5.18 Measured TX-factor based on differential thermocouples.

Figure 5.19 Daily variation of the simulated temperatures using FEM.

Especially during the summer period the TX-factor shows daily variations. This is also confirmed from the thermistor measurements. This variation is not well understood as the infrared results do not show the same variations. Finite Element (FEM) simulations also show much less daily variations. However, the FEM simulations do confirm that inaccuracies in the location of the temperature sensors can cause very

large daily variations due to the time lag in the vertical heat transfer, Figure 5.19. This probably is also the cause for the large fluctuation of the long-term measurements with thermocouples.

In September 1994, several sets of IR measurements were made on the test field. Both the US and the Finnish participants used their own IR equipment to make these measurements. According to Figure 5.12, the pipe temperature was 35ºC and the measured heat loss ca 90 W/m. The TX factor measured with both camera systems (Inframetric and AGA Thermovision 782, respectively) were 4.2 ± 0.4. Figure 5.18 shows an average value of about 4, but with very high fluctuations for the reasons mentioned above. From equation (15) we expect a heat loss of about 80 - 90 W/m depending on the wind which was not known very accurately, but estimated to about 3 m/s. Thus the agreement between the measured heat loss and those predicted by the TX method is good.

Hence we can conclude from the measurements in Lyngby that the TX factor can be used even for measuring on cooling pipes, rendering negative TX factors. However the Interpretation Models derived to date are not applicable and verified for cooling conditions. Furthermore we could state that IR measurements showed reasonable agreements compared with results from ATXIM1. On the other hand, field measurements with temperature sensors proved to be problematic. Similar to the experience at Studsvik, it was found that fluctuations can be large because of experimental imperfections. Thus it can be concluded that IR measurements are the preferable source for quantitative heat loss determination based on the TX method.

5.3 EXPERIMENTS IN LAPPEENRANTA, FINLAND

The heat loss experiments were made in Lappeenranta during the period from 1984 to 1986. The temperature readings were measured from the temperature sensors in the ground and on the surface. The test field was built for research purposes and was not connected to the normal district heating system. The lines were electrically heated and the heating energy was measured. Temperature in the pipes was controlled by electrical heaters according to the outdoor temperature. It should be noticed that the ground surface temperature measurements does not in all cases accurately yield the same temperature as infrared measurements, as was noted in the results from Denmark and Sweden discussed above.

The test pipeline consisted of six different distribution line types, two of which were selected here for the TX-calculations, as shown in Figure 5.20.

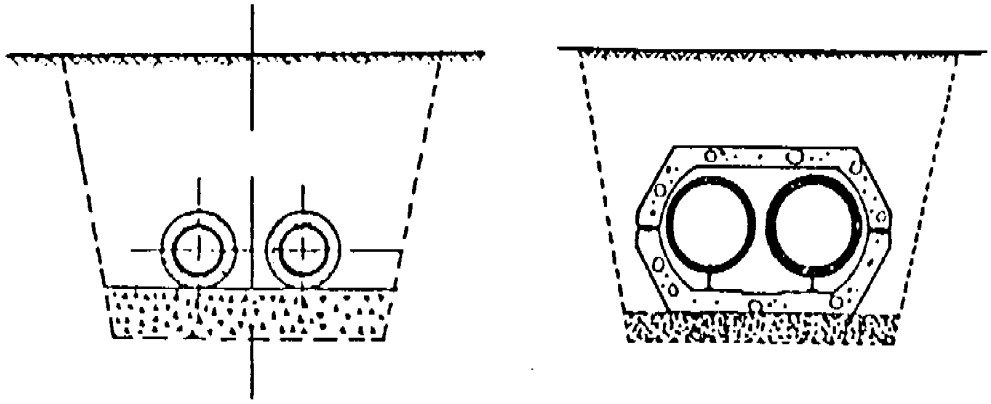

Wehotherm Standard Partek

Figure 5.20: Two different duct types evaluated with surface temperature measurements.

Table 5.1 Technical data.

Duct	Wehoterm Standard	Mineral wool (Partek)
Depth of the duct	0.83 m	0.65 m
Horizontal distance	0.3 m	0.24 m
Ambient temperature	10.4 °C	12.9 °C
Thermal conductivity of soil	1.6 W/(m°C)	1.6 W/(m°C)
Steel pipe:		
Outer diameter	114.3 mm	114.3 mm
Inner diameter	107.1 mm	107.1 mm
Wall thickness	3.6 mm	3.6 mm
Insulation:		
Insulating material	polyurethane (80 kg/m^3)	mineral wool

Insulation thickness	64 mm	supply pipe 60 mm, return pipe 40 mm
Cover:	Plastic pipe 250 mm	Concrete culvert

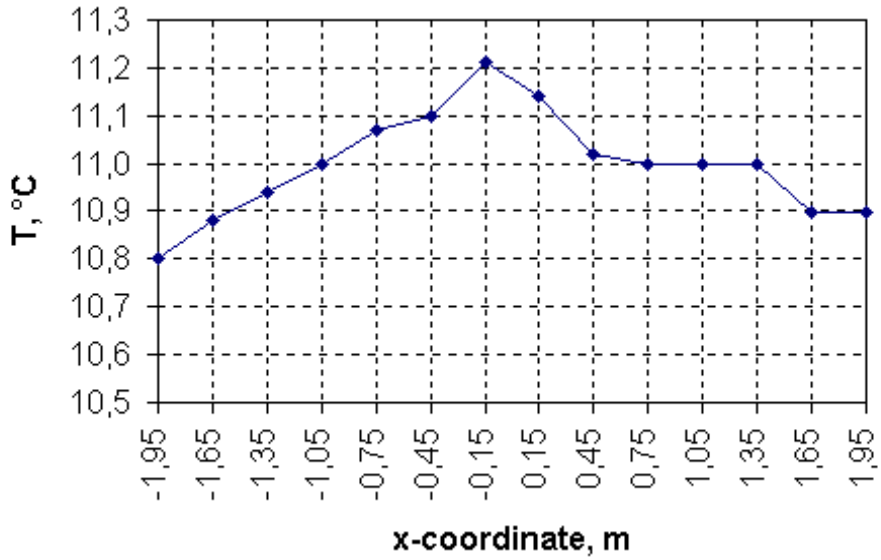

Figure 5.21 Wehotherm Standard: Temperature profile of the ground surface. TX = 0.81 [°C·m].

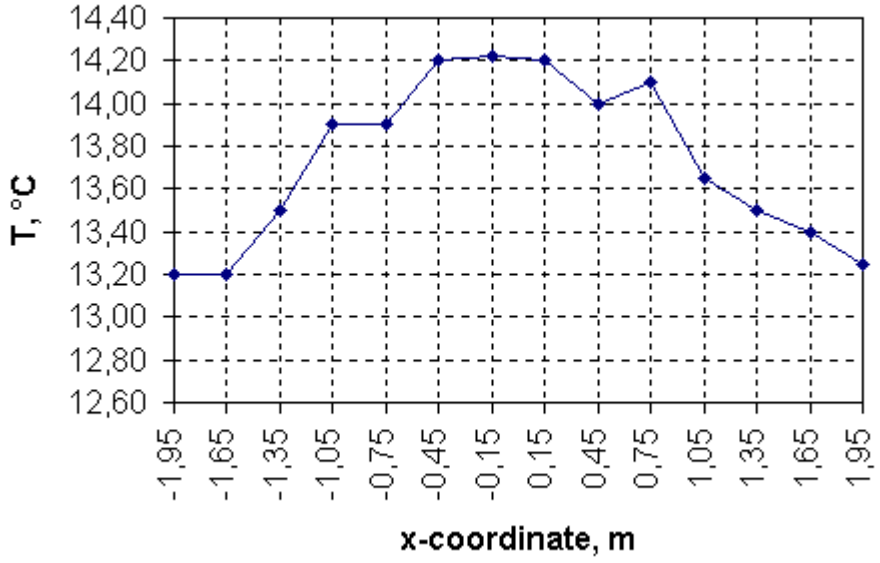

Figure 5.22 Concrete duct: Temperature profile. TX = 2.22 [°C·m].

Table 5.2 Heat losses from the ducts.

	Wehotherm	Partek
Measured heat loss, W/m	21.8	42.5
TX-calculation, W/m	24.2	40.5

Hence the results from Laappeenranta show, contrary to the results from Studsvik and Lyngby, that there is also a good agreement in the chosen examples between measured heat loss and ATXIM1 evaluation based on temperatures measured with temperature sensors. This holds also for an alternative piping design, i. e. the concrete duct of type Partek.

5.4 EXPERIMENTS IN FT. JACKSON, USA

The Department of Defense of the United States has an active research program in district heating technology. The objective of this program is to identify improvements in methods and systems which will prove to be less costly and problematic. The initial instrumentation portion of the work described here was funded by this program. Ft. Jackson, South Carolina was selected as a site because a project replacing a major portion of the distribution network was underway there. Three types of buried heat distribution piping systems were installed:

1. Shallow concrete trench with top cover at grade level,
2. Steel conduit system with supply and return piping in a common conduit, and
3. Steel conduit system with supply and return piping in individual conduits.

The specifics of each of these types of construction can be found in Phetteplace et al., 1991. The instrumentation installed on each system is also described in that report. Initially it was hoped that both of the sites with the steel conduits could be used in this study of the TX method, but upon making field trials at the sites it was found that the individual conduit site was buried too deeply for us to obtain a reliable temperature profile at the ground surface, which was covered with grass. An attempt to measure the temperature profile of the shallow concrete trench was also made, but it was determined to be an unacceptable application of the TX model as currently developed. For this reason, only the results from the steel common conduit site are discussed below.

5.4.1 Site Description

The common conduit system has both the supply and return piping in the same steel conduit, see Figure 5.23. The conduit system used at Ft. Jackson consists of schedule 40 steel supply and return pipes of 5 inch(~125 mm) nominal pipe size (NPS). These pipes are insulated with a mineral wool insulation of 1.5 inch (38 mm) thickness. The insulated supply and return pipes are encased in a spiral-wound steel conduit which is approximately 1/8 inch (3.2 mm) thick. The supply and return pipes are oriented vertically within the conduit with the supply pipe on top of the return pipe. The conduit has an outer diameter of approximately 20 inches (~500 mm), thus allowing for an air space between the pipe insulation and inside of the conduit. The conduit is covered with a asphalt-based corrosion resistant coating. All field closures of the conduit are welded and coated. The interior air space between the pipe insulation and the conduit inner diameter is designed to be drainable and dryable. The integrity of the air space can be checked by pressure testing at 15 psi (~1 bar).

Heat losses from the instrumented systems at Ft. Jackson have been measured over a period of several years starting in 1986. Thermocouples have been used to make temperature measurements which allow the computation of heat losses by several different methods. Figure 5.24 shows the locations of the thermocouples in and on

the conduit and in the soil around the conduit. Control temperatures were also measured in undistributed soil at various depths. Using the measured temperature data we are able to calculate heat losses using the methods outlined in Phetteplace et al., 1991.

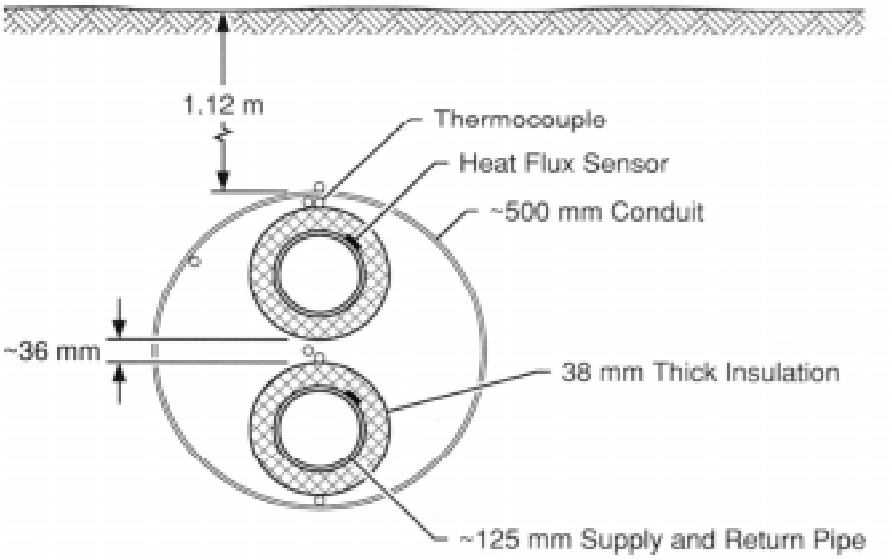

Figure 5.23 Common conduit site.

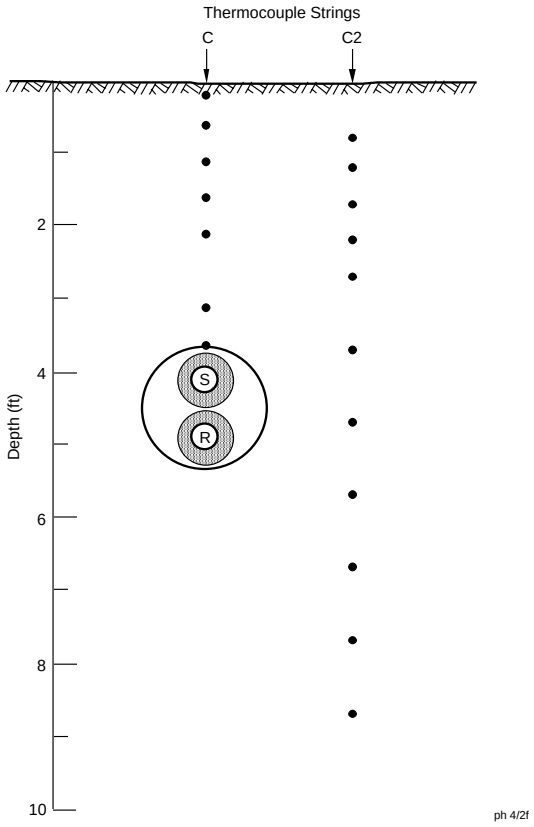

Figure 5.24 Common conduit site instrumentation.

5.4.2 Infrared Measurements

Our objective of these tests was to compare the heat loss rate as measured by the installed instruments with that which would be obtained by using the TX factor method. Our infrared measurements used to compute the TX factor were made using an AGA Thermovision 782 infrared scanner. This system was used from the ground surface mounted on a hand cart for portability. The scanner was positioned on a support pole that placed the scanner approximately 3 meters above the ground surface. The signal conditioning of the AGA Thermovision 782 system does not allow for the direct determination of the temperature profile needed to compute the TX factor. Thus, it was necessary to use a human as a spotter for successive isotherm locations with respect to the centerline of the pipe. This procedure is time consuming but appears to yield acceptable results. Most infrared scanners which have been manufactured in recent years have the necessary signal processing to directly yield the temperature profile needed for the TX factor computation.

A secondary objective of our measurements at Ft. Jackson was to evaluate different types of surfaces to see what effect they would have on TX factor measurements. At Ft. Jackson the instrumented pipeline passes under a concrete sidewalk in a perpendicular orientation at a location immediately adjacent to the location of the instrumentation. The concrete sidewalk was thus used as one of the surfaces for the TX factor measurements. Three other surfaces were evaluated by covering the grass adjacent to the side walk. Two separate trips were made to Ft. Jackson to make the field measurements. During the first set of tests we evaluated the concrete surface as well as surfaces of loose soil and asphalt shingles. During the second set of tests we evaluated the concrete sidewalk and asphalt shingles a second time as well as a thick rubber sheet and the native grass itself. Each of these test surfaces was approximately 1 meter wide and oriented perpendicular to the axis of the pipeline. The asphalt shingle surface consisted of several layers of asphalt roof shingles as would be used in residential home construction. These layers were staggered and the shingles were inverted so that the smoother underside was exposed for the infrared measurements of the TX profile. In each case, when evaluating the test surfaces we would place them at least 6 to 8 hrs before the temperature profile measurements were to be made. This allowed the test surface achieve a temperature distribution similar to that of the actual ground surface underneath it. Wherever possible, we also repeated the measurements with the infrared scanner positioned at two different distances from the test sections to see what effect scanner angle and perspective might have. The first set of measurements were made on 18 August 1994. The surface temperature profiles measured by the infrared scanner for the first set of tests are shown in Figure 5.25 a, b, c. Table 5.3 gives the TX factors calculated from the temperature profiles of these Figures 5.25 a, b, c.

The second set of tests were conducted on 28 January 1995. Because it began to rain before we could conclude all our testing on this date, we were unable to obtain temperature profiles at differing scanner distances as had been done in some of the earlier tests. The surface temperature profiles for these tests are shown in Figures 5.26 a, b, c, d. The onset of rain also prevented us from obtaining a complete tem-

perature profile for the rubber sheet, see Figure 5.26 d. The TX factor for this case was calculated by taking the area under the temperature profile assuming that the outside edges of the profile are vertical to the X-axis.

5.4.3 Measured results

From the measured TX factors the heat loss can be calculated using the interpretation model ATXIM. Using the two interpretation models discussed in Chapter 6 (Equations 15 and 16) the heat losses have been calculated for the TX factors measured at Ft. Jackson. In Table 5.3 the results of the heat loss calculations from the TX factor are compared with the heat loss measured using the methods described in Phetteplace et al. 1991. The comparison is quite favourable when averaged over all the surfaces used to make the TX factor measurements with the TX factor method underestimating the heat losses by approximately 13% for the two separate sets of measurements made at different times. Table 5.3 shows that the effect of the choice of TX model, i.e. Equation 15 or 16, appears to have little effect on the calculated heat loss results for the conditions prevailing for the tests at Ft. Jackson.

For the first set of tests the results from the TX factor method applied to the various surfaces ranges from about 17.6% underprediction for the concrete sidewalk surface to 11.5% over- prediction for the asphalt shingle surface. The bare soil surface performed the best with the TX method underpredicting the measured heat loss by 8.4%. For the concrete sidewalk and asphalt shingle surfaces, the infrared measurements of the temperature profile were made with the camera positioned at two different distances from the test surfaces. The variation in results was significant for the concrete sidewalk surface while for the asphalt shingles much less variation was noted.

For the second set of tests the results from the TX factor method applied to the various surfaces ranges from about 3.5% overprediction for the concrete sidewalk surface to 24.2% underprediction for the grass surface. The concrete sidewalk surface performed the best with the TX factor method under predicting the measured heat loss by 3.5%. Unfortunately, because it started to rain it was not possible to conduct a second series of tests with the infrared camera positioned at a different distance from the test sections as had been done in the first set of tests.

The advanced TX factor interpretation models given by Equations 15 and 16 were formulated based on numerical simulations where the integration half-width was 2.5 m or less. In a number of our field trials at Ft. Jackson our temperature profiles exceeded this width. This deviation from the proposed range for the interpretation models was not accounted for in any way in the results presented in Table 5.3. To see what effect this might have we repeated the calculation of the TX factors for the Ft. Jackson field tests but limited the integration half-width to 2.5 m. This was done by neglecting any contribution to the TX factor which would result from integrating the temperature profile beyond the 2.5 m half-width. Table 5.4 shows the results from these calculations. These results are not significantly different from those obtained using the full width of the temperature profile as measured.

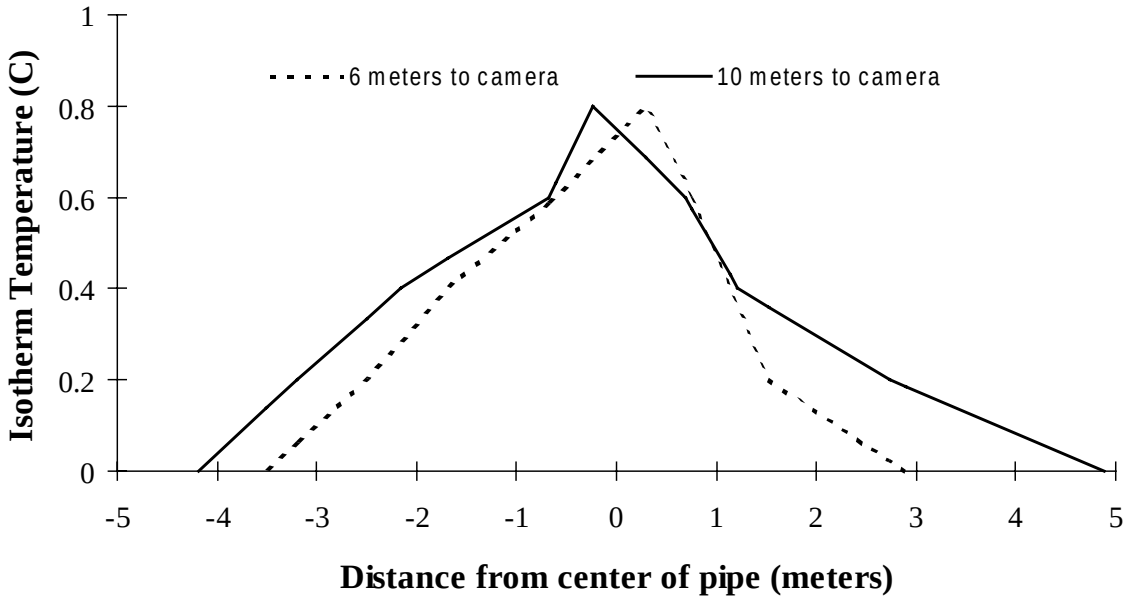

Figure 5.25a Ft Jackson, Concrete Sidewalk, 18 August 1994.

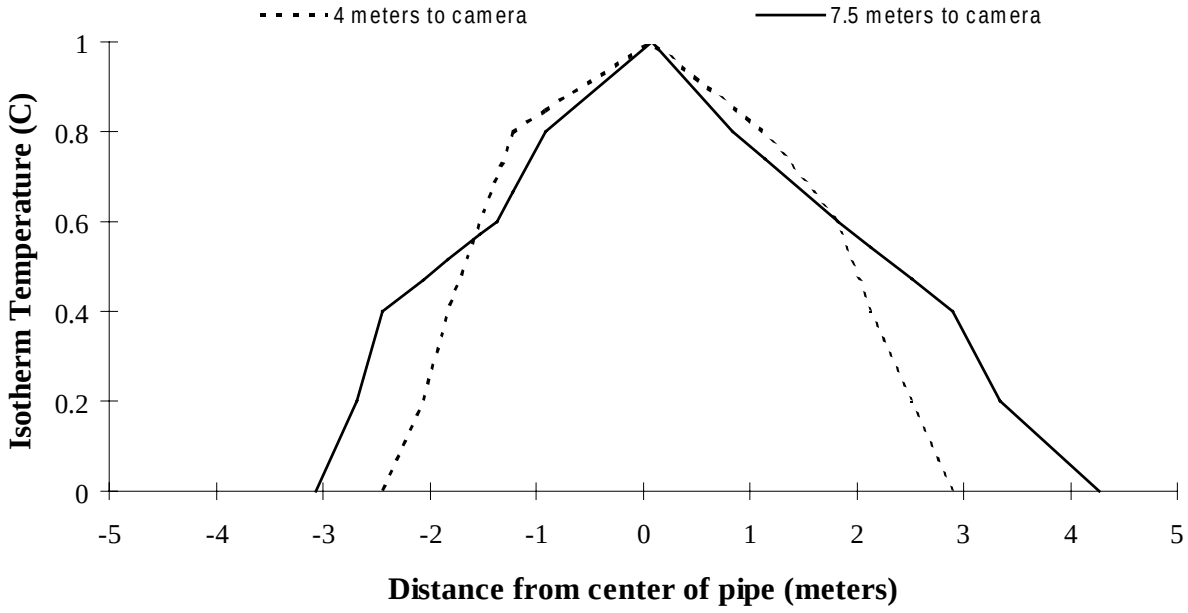

Figure 5.25b Ft. Jackson, Asphalt Shingles, 18 August 1994.

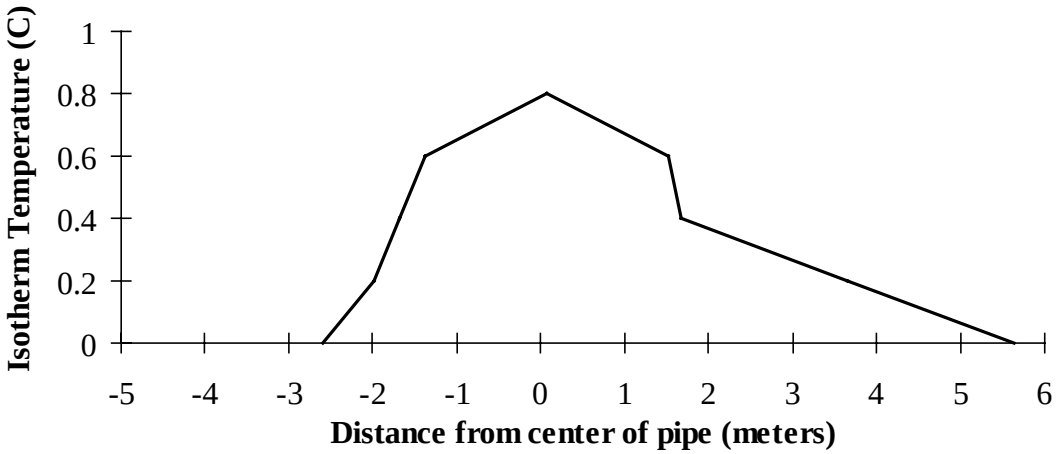

Figure 5.25c Ft. Jackson, Soil, 18 August 1994.

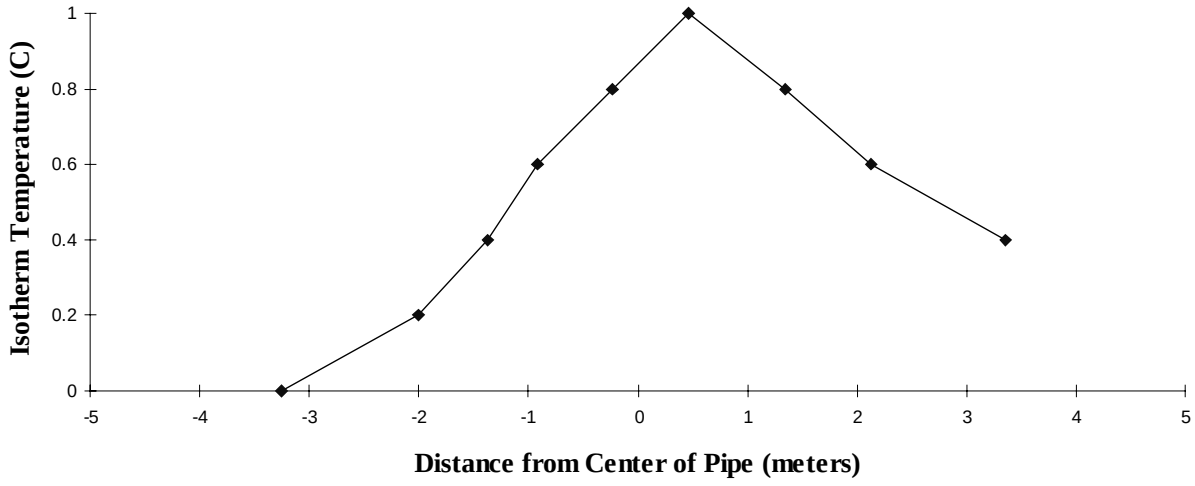

Figure 5.26a Ft. Jackson, Concrete Sidewalk, 28 January 1995.

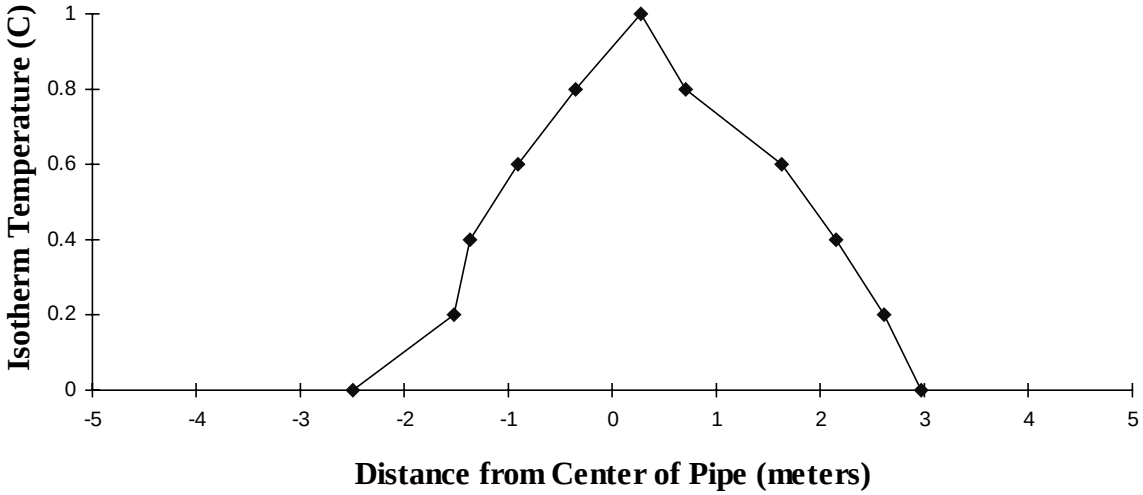

Figure 5.26b Ft. Jackson, Asphalt Shingles, 28 January 1995.

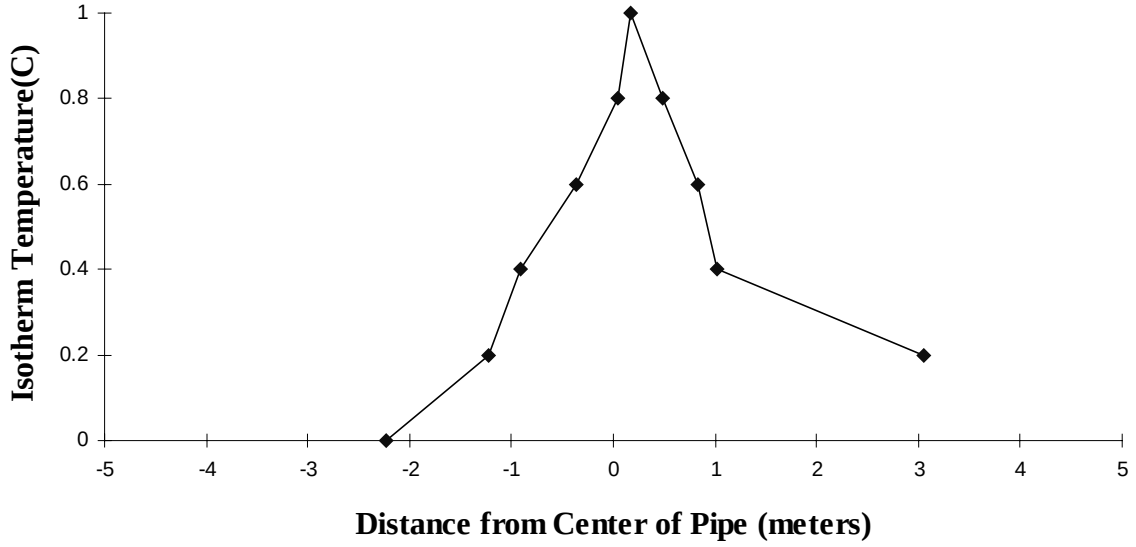

Figure 5.26c Ft. Jackson,Grass, 28 January 1995.

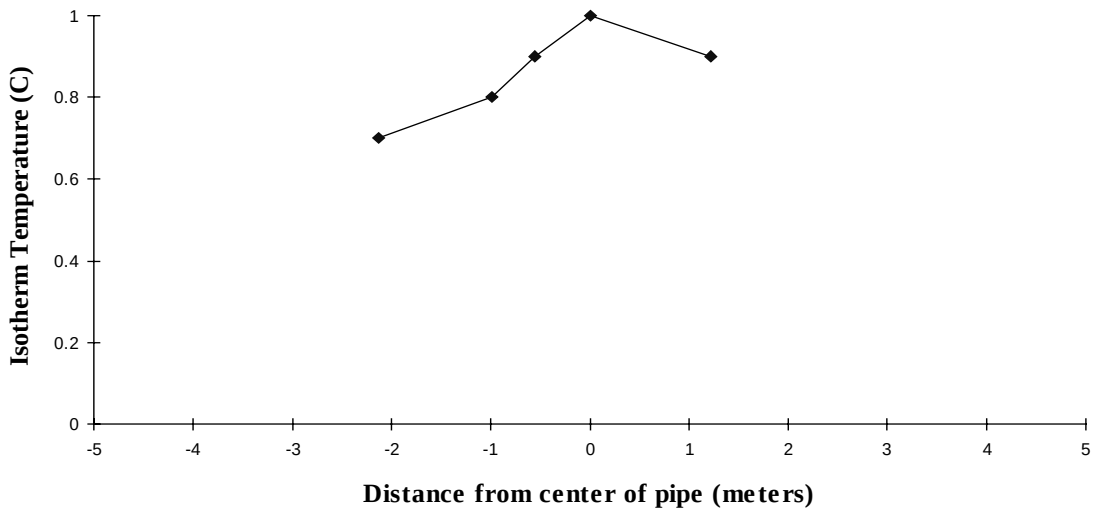

Figure 5.26d Ft. Jackson, Rubber Sheet, 28 January 1995.

The TX factors calculated using the temperature profiles from the second set of tests are given in Table 5.3.

5.4.4 Observations and conclusions.

The TX factor method appears to provide a reasonably accurate estimate of the heat losses. This is confirmed by the results from the other field tests described earlier in this report. Surface type has a significant impact on the effectiveness of the IR surface temperature measurements. The soil surface had the best test results with the average error for the two models being only 8.4%. However, only one test was conducted on the soil surface, thus this result is felt to be inconclusive. Other than the isolated soil surface result, the asphalt shingle surface had the best results when averaged over all three tests and both models with the average error being only 10.3%. The concrete sidewalk surface performed essentially equivalent to the asphalt shingles with the results averaged over all three tests and both models having an average error of 12.9%.

The results from the single rubber sheet test were inconclusive. It was difficult to discern the isotherms when using the rubber sheet. More work is needed with this surface to see if it could be an acceptable expedient alternative for placement over grass surfaces. The test results for the grass were the worse of all the surfaces tested. The grass in this area was quite thin leading one to believe that in instances where the grass is thicker IR measurements might be impossible altogether. It is important to note, however, that in all of these test the heat distribution pipes were

in good condition with normal heat losses. Where heat losses are elevated due to system

Table 5.3 Ft. Jackson TX factor test summary.

Date	Surface	Distance to Camera (m)	TX Factor (m°C)	TX Factor half-width (m)	Q model 1 (W/m)	Q model 2 (W/m)	Q measured (W/m)	Error model 1 (%)	Error model 2 (%)
18 August 94	Concrete	6	2.28	3.20	82.3	80.7	103.5	20.5	22.1
18 August 94	Concrete	10	3.04	4.53	89.9	88.1	103.5	13.1	14.9
18 August 94	Asphalt Shingles	4	3.38	2.67	116.2	113.6	103.5	12.3	9.8
18 August 94	Asphalt Shingles	7.5	4.00	3.67	117.1	114.5	103.5	13.2	10.6
18 August 94	Soil	5	3.20	4.12	95.8	93.8	103.5	7.4	9.4
18 August 94	**Average all surfaces**	----------	**3.18**	**3.64**	**100.3**	**98.1**	----------	**13.3**	**13.3**
28 January 95	Concrete	6.7	3.60	3.30	119.0	119.2	115.1	3.4	3.6
28 January 95	Asphalt Shingles	3.81	2.80	2.73	105.9	106.1	115.1	8.0	7.8
28 January 95	Grass	5.18	20.9	2.64	87.2	87.4	115.1	24.2	24.1
28 January 95	Rubber Sheet	3.05	2.91	1.68	135.8	136.0	115.1	18.0	18.2
28 January 95	**Average all surfaces**	----------	**2.85**	**2.59**	**112.0**	**112.2**	----------	**13.4**	**13.4**

system failures, higher heat losses will enhance the viability of the surface temperature signature. This observation is substantiated by our personal experiences looking for problem areas in a qualitative manner with the IR camera. We have been able to locate problem areas under grass in a few instances and have successfully located a number of problem areas under bare soil surfaces as well as concrete and asphalt pavement surfaces.

Table 5.4 TX factor results for integration half-width limited to 2.5 m.

Surface	Distance to Camera (m)	TX Factor (m°C)	Q model 1 (W/m)	Q model 2 (W/m)	Q measured (W/m)	Error model 1 (%)	Error model 2 (%)
Concrete	6	2.17	91.3	91.5	103.5	11.8	11.6
Concrete	10	2.49	100.7	100.8	103.5	2.7	2.6
Asphalt Shingles	4	3.34	125.4	125.7	103.5	21.2	21.4
Asphalt Shingles	7.5	3.51	130.4	130.6	103.5	26.0	26.2
Soil	5	2.7	106.8	107.0	103.5	3.2	3.4
Average all surfaces	----------	**2.84**	**110.9**	**111.1**	----------	**13.0**	**13.0**
Concrete	6.7	3.2	121.4	121.6	115.1	5.4	5.6
Asphalt Shingles	3.81	2.74	107.9	108.1	115.1	6.2	6.0
Grass	5.18	1.97	85.5	85.6	115.1	25.7	25.6
Rubber Sheet	3.05	----------	----------	----------	----------	----------	----------
			-	-			--
Average all surfaces	----------	**2.64**	**104.9**	**105.1**	----------	**12.5**	**12.4**

6 The advanced heat loss interpretation model

In principle, the simulation model described in Chapter 3 can be used for determining the heat loss from pipes. It is expected to give very precise results for all types of pipes and for many different climate situations during the year, but it also requires a large amount of input information and computing power. Therefore in Jönsson, Zinko (1992), a simple interpretation model which converts the temperature profile from a thermograph to an instantaneous heat loss from the district heating pipes was proposed.

Our aim is to extend this model to include also the principal findings of this report, i.e. the influences of wind and changing surface temperatures. This model will then be called "Advanced TX heat loss interpretation model" ATXIM. The final goal is that this interpretation model can be integrated in the thermographic diagnostic devices for heat loss determination.

The variation of the TX factor during the summer time was shown in Chapter 4 for the simulated field conditions in Studsvik. In Chapter 5 the influence of some parameters on TX have been discussed. The simulations based on hourly climate data showed more or less strong fluctuations of the TX factor. It turned out that the strongest variation of the TX factor is due to the wind. For low winds, as experienced during the period of IR measurements at Studsvik, relatively low fluctuations that reflect the changes in the surface temperature are expected. They are indeed not very strongly expressed in the measurements (see Figure 5.9).

The problem in establishing the new ATXIM including wind and temperature fluctuations was that of extending the multiple linear regression model of Equation (8) with the influences of wind and surface temperature variations. By doing that with the climate of 1986 for Stockholm, it turned out that the linear regression model did not result in a stable solution. Hence we looked at an exponential regression for the change in the surface temperature and the wind and found the following solution for the reference case (= Studsvik conditions, 54 W/m):

$$TX_{mod} = TX(w,T_s) = 1.68 + 2.36 \cdot (0.8)^{<w7>} - 0.33 \cdot <T_s14>/<T_s24> \qquad (12).$$

Equation (12) combines the influence of wind and changing surface temperature. Whereas the wind is considered to be an independent variable, the influence of the surface temperature is dependent on the wind and only important for small winds below 1 m/s. For larger winds, the temperature fluctuations are overshadowed by the fluctuations caused by the wind. Equation (12) can for stronger winds be simplified to Equation (13). See also Figure 6.1.

$$TX_{mod} = TX(w) = 1.34 + 2.35 \cdot (0.8)^{<w7>} \qquad (13).$$

<w7> is the mean value of the wind during the last 7 hours.

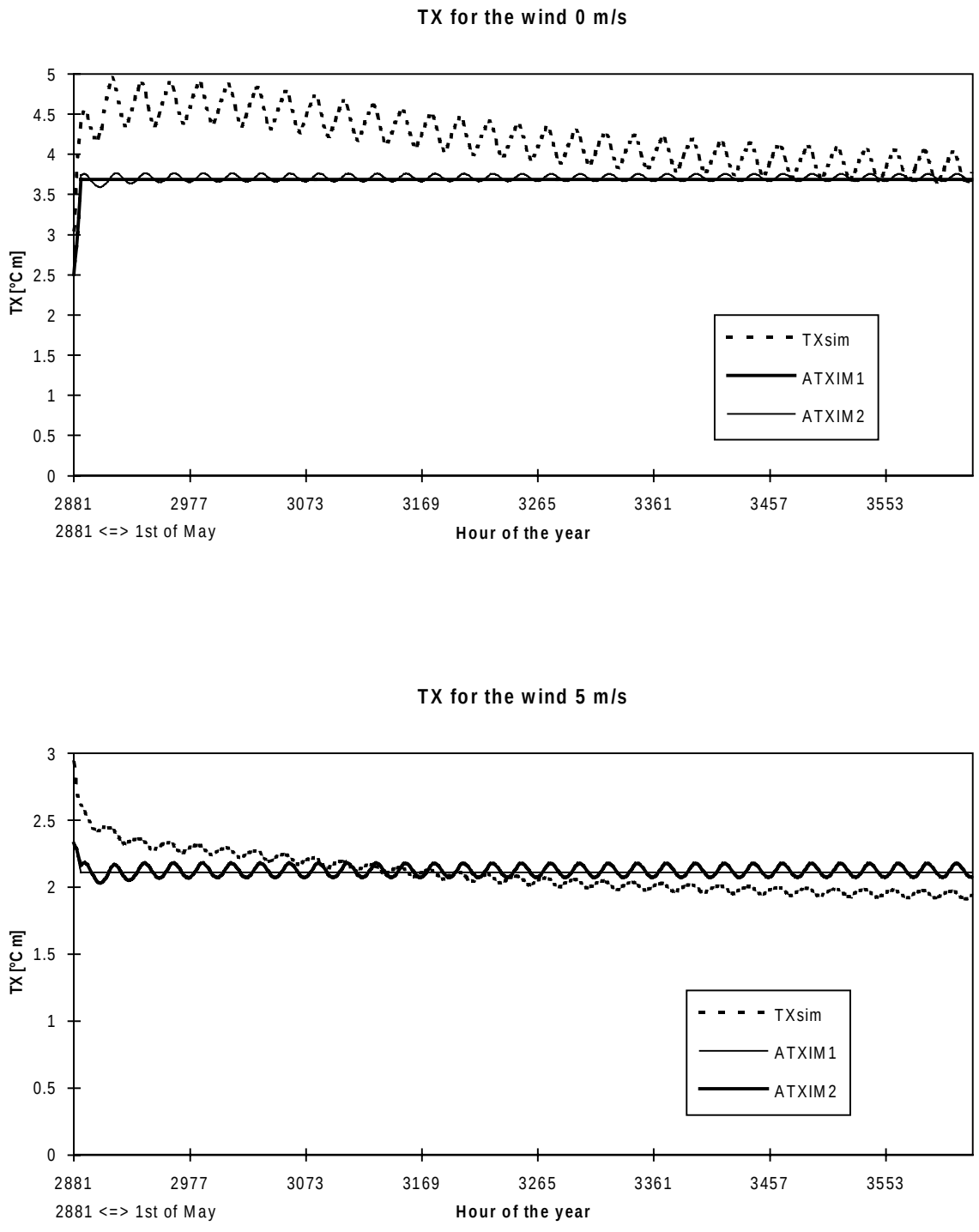

Figure 6.1 TX factor for small wind and large wind according to Equations (12) and (13). The heat loss from the pipes is in both cases 54 W/m.

Hence the advanced interpretation model ATXIM is proposed as a combination of the old interpretation model and a modified TX_{mod} which now includes the wind and the surface temperature variations.

$$P_f = TX_{meas} \cdot [\, 2.5/TX_{mod} \,] \cdot [-13.6 + 19.6 \cdot h_f + 4.3 \cdot \lambda + 12.8 \cdot (dT_m/dt) + 40.1/x_m] + \\ + 9.1 \cdot h_f - 6.3 \cdot \lambda + 18.8 \cdot (dT_m/dt) + 24.7/(x_m)^2 \qquad (14)$$

with

h_f = the depth of the pipe trench, m

λ = the thermal conductivity in the ground, W/(m·K)

dT_m/dt = change of mean distribution temperature during the last weeks, °C/24 hours

x_m = the distance in each direction from the center of the pipes to the end of the temperature profile, m

$<w7>$ = The average wind velocity during the last 7 hours, m/s

$<T_s14>$ = Mean ground surface temperature during last 14 hours, °C

$<T_s24>$ = Mean ground surface temperature during last 24 hours, °C

In many cases, especially for winds above 1 m/s the surface temperature dependent term can be omitted and the ATXIM is reduced to ATXIM1:

$$P_f = TX_{meas} \cdot [2.5 /(1.34 + 2.35 \cdot (0.8)^{<w7>})] \cdot [-13.6 + 19.6 \cdot h_f + 4.3 \cdot \lambda + \\ 12.8 \cdot (dT_m/dt) + 40.1/x_m] + 9.1 \cdot h_f - 6.3 \cdot \lambda + 18.8 \cdot (dT_m/dt) + \\ 24.7/(x_m)^2 \qquad (15)$$

For the case of low winds, a correction term for the change in the surface temperature can be included and ATXIM2 reads then:

$$P_f = TX_{meas} \cdot [\, 2.5 /(1.68 + 2.36 \cdot (0,8)^{<w7>} - 0.33 \cdot <T_s14>/<T_s24>) \,] \cdot \\ [-13.6 + 19.6 \cdot h_f + 4.3 \cdot \lambda + 12.8 \cdot (dT_m/dt) + 40.1/x_m] + 9.1 \cdot h_f - 6.3 \cdot \lambda + \\ 18.8 \cdot (dT_m/dt) + 24.7/(x_m)^2 \qquad (16)$$

By means of the simulations model, the parameters have been varied within the following limits, which also is the limit of validity for the approximation:

h_f :	0.5 - 1.0 m
λ:	0.5 - 2.0 W/(m·K)
$x_{m:}$	1.5 - 2.5 m
dT_m/dt:	± 0.16 °C/(24 hours) (= 5°C maximal change in one month)
w:	0 - 10 m/s
$T_{s:}$	0 - 50 °C.

Figure 6.2 summarises these findings by comparing the TX factor for Stockholm 1986 with the results of the ATXIM including wind (ATXIM1) and wind and surface temperature (ATXIM2). As it can be seen, the agreement between these three curves is quite satisfactory.

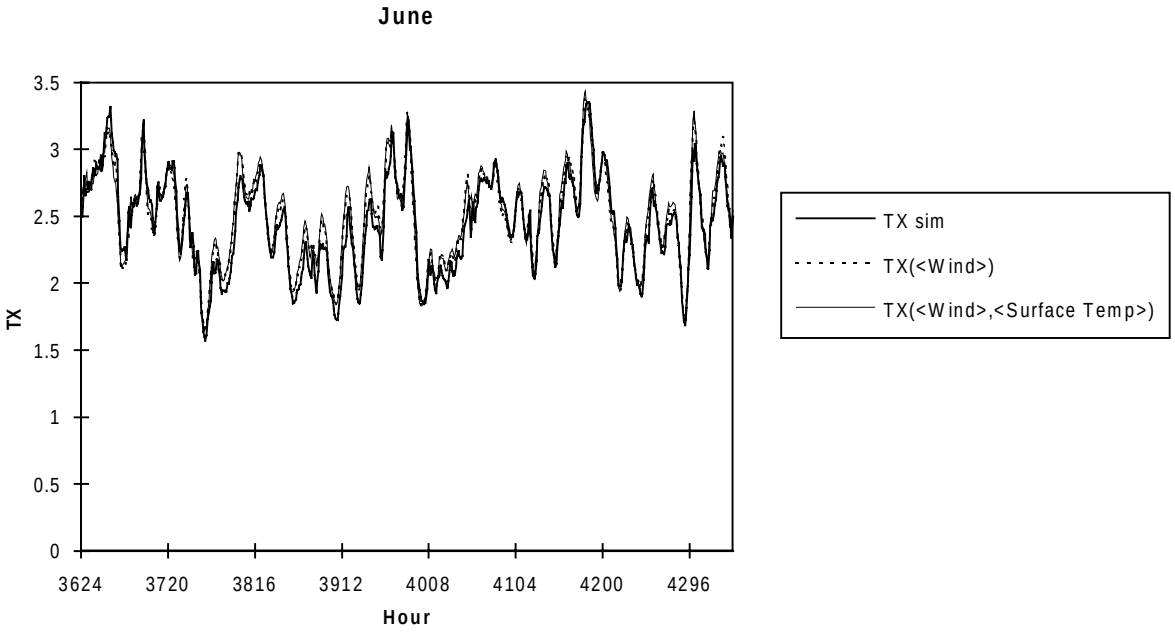

Figure 6.2 TX factor for Stockholm 1986 according to simulation model and ATXIM2 and ATXIM1, including wind and surface temperature as well as only wind, respectively.

7 The range of applicability of the TX model

It should be noted here that the TX model expressed in the Advanced Interpretation Model ATXIM is an ***semi-empirical model*** intended to be used within a defined range of boundary conditions. In this case the term "semi-empirical" means that the model is not analytically derived but well based on simulation results from a reasonable heat transport model for both the ground and the ground surface. Some of the simulated conditions could be verified with field measurements, but many conditions have not been tested. The equations (15, 16) for the TX model are results from multiple regression analyses and do not represent physical descriptions.

Two kinds of conditions exist which have a major influence on the applicability and the accuracy of the ATXIM:

- *The properties of the soil and the ground surface*
- *The climat*e.

In this chapter we will discuss these influences and the limitations they pose on the applicability of the model.

7.1 THE PROPERTIES OF THE GROUND AND THE GROUND SURFACE

Ground conditions

An important conditions is the *uniformity* of the ground and the ground surface. As shown in Chapter 4, the TX factor is not very sensitive to variations within certain limits of the heat capacity C and thermal conductivity λ of the soil (see Figure 4.7). A small correction is given in the ATXIM. Figure 4.4 shows the influence of the non uniform ground on the TX factor by means of a simulation, in which the sandbed is varied in respect to that of the surrounding soil. Even in the worst case of a trench filled with sand and surrounded by rocks (granite), as it could be the case in Sweden, no strong influences on the TX profile can be observed, if the top layer consists of uniform asphalt. Singular inclusions such as large stones or ducts in the earth might be seen as week bumps in the TX profile.

The *depth h_f of the pipes* has been shown to be a very important parameter for the value of the TX factor. The model was tested to work for h_f between 0.5 and 1.1 m and by means of simulations the applicable depth was extended to 1.25 m. However the TX factor decreases strongly with depth as shown in Figure 4.19 and the error might become larger than 30% at depth below 1 m. ***It is very important to know the burial depth h_f of the pipes as precisely as possible.*** If h_f is not known from drawings, or if it can be suspected that the depth of the pipes has been changed (i. e. by

adjusting street levels or by adding new asphalt layers), the buried depth of the pipe should be measured. This can be done, for example, by means of available electronic detection devices.

In experiments the suitable integration width was found to be between 3.5 and 5 m. One might suspect a correlation between integration width and depth, larger depth calling for larger width. We could not establish this connection experimentally, but from simulations it was found that the ranges 1.5 m < X < 2.5 m for the integration width and 0.5 m < h_f < 1.25 m for the depth give a suitable freedom.

Surface conditions

An important role is played by the conditions of the uppermost 20 cm closest to the *ground surface* and the properties of the surface. This layer should be as uniform as possible at least across the integration width 2X. A flat asphalt layer, such as that found at the Studsvik test field and also in the middle of many streets, is an ideal surface for TX measurements. Concrete tiles, dry sand surfaces and asphalt shingles have also been used as reference surfaces. Figure 4.5 shows the consequences of an abrupt change of the thermal conductivity in the top layer, as it is the case on the border of a street. The TX profile is disturbed at the boundary and an useful TX value cannot be defined.

Shadows on the surfaces disturb the profile. The surface should not be partially shadowed from direct sunlight for at least one hour preceding the measurement of the TX profile. Uniform shadowing should not present a problem if it exists for at least one hour prior to the measurements. The absorption coefficient of the ground's surface should be high (> 0,7) and also uniform. Reflecting and metallic surfaces are not suitable for TX measurements.

Grass surfaces are not suitable for TX-evaluation. This results from the fact that grass forms an insulating layer on the ground and its IR signature is a function of the moisture and temperature of the blades of grass. Hence the IR image of the grass does not reflect the ground temperature and the TX profile does not correlate with the heat loss. Experiments with rubber sheets on grass did not work well, partly because of the remaining air space inside the grass. In the tests performed by the US contributor to this study (see section 5.4) asphalt shingles performed well when layed over grass. We attributed this to their weight being great enough to compress the grass significantly and also their ability to conform the ground nicely. In these same tests a layer of top soil placed on the grass also performed well. Presumably a layer of sand or perhaps concrete tiles on the grass would also work well. Unfortunately most of these alternatives are cumbersome, some more so than others.

Unknown or non uniform surfaces (other than grass) can be covered with a reference surface. Asphalt shingles (usually for sale as a roof cover) should also work very well for this purpose. The cover surface should be heavy for good thermal contact and not to large in order to avoid air to be locked between cover and ground. Asphalt shingles were shown to be very suitable for that. A larger rubber

sheet (2m × 6 m × 1.5 mm) was also tested, but failed because of bad contact to the ground.

Stable pipe temperatures. The TX factor measured at a given time represents the insulation status (and temperature condition) from a period starting about one week prior. Hence, changes in the insulation status which are more recent than this, can not be correctly analyzed. Similarly, if the distribution temperature has changed drastically within the preceding week or so, one must be careful in interpreting the thermography results.

7.2 CLIMATE

It should be clearly stated here that the night and cloudy weather during the day are the most suitable conditions for quantitative heat loss measurements by means of the TX model. *However, it has been shown that even sunny summer days can be used for TX evaluations.* The only restriction in this case is that the irradiation must have been uniform for at least the last hour before the measurement. This means that the area around the measurement line should either have been fully exposed to the sun or completely in the shadow.

*The influence of the wind is an important parameter and is included in the TX model. A*s it is described in Chapter 4, the wind has a tendency to cool the ground and thus flatten the TX profile. The wind influences not only the surface, but also through thermal conduction the top ground layer a few centimeters down. It has been found that the wind conditions of the last 7 hours have an influence on the TX factor and a mean value for this period should be included according to the ATXIM. We recommend that for quantitative evaluation the wind speed measured at 5 m height should be below 10 m/s.

Frozen ground conditions are not acceptable. The heat transfer in the ground is disturbed by
the latent heat of moisture in the soil and the TX factor can vary widely as a result. Hence the winter periods, when freezing of the ground occurs in many areas with district heating, are **not** useful for TX evaluation.

Wet and drying surfaces will not work. A reduced TX profile can be measured under wet surface conditions (see Figure 4.15). However for making a quantitative analysis, one needs to know the thickness of the water layer on the surface and the evaporation rate. The evaporation of water involves latent heat and hence will disturb the temperature profile. Of course snow cover on the ground is not acceptable at all either.

Simulation made with typical Swedish and Danish climates showed (Figure 4.1 and Figure 4.2) that it is possible to use the TX method from May to end of October in Middle Sweden and from April to end of November in Denmark. If from these periods we subtract rainy periods, and add some margins for drying surfaces, we esti-

mate some 3000 useful hours are available for TX evaluation in Sweden and about 4000 useful hours are available in Denmark.

7.3 MEASUREMENT PROCEDURE

With modern equipment, manufactured for example by AGEMA or INFRAMETRICS, the measurement procedure is simple but involves some discrete steps. Currently the method is most suitable for evaluation of well defined measurement sites prepared in advance. However, we can easily foresee the development of a standard procedure for quantitative heat loss measurements based on this method.

Preparation of measurement positions and IR-measurements

- Investigate climate conditions sun, rain, wind and so on. Can you get a wind record for the hours before measurements or can you measure the wind yourself?

- Plan the measurements by selecting areas with uniform surfaces. Consider irradiation conditions, humidity, wind, possible shadows.

- Get information about the burial depth of pipes and the soil conditions. Consider possible nonuniformities in the ground such as crossing lines or pipes, water channels, chambers, etc.

- The camera angle should not be too low, i.e. > 25°. Choose the correct lens and prepare a method to obtain the proper distance (with a wide viewing angle of 40° and a height above ground of 2.5 m, a distance of about 6 m is necessary between camera and measurement position.

- Make marks at the ground for indicating the X line (place for instance small metallic rods parallel to the pipe axis just at the ends of the chosen X line.

- Adjust the camera according to the instructions (compensating for ambient and sky temperature, absorption and emission factors of the ground). If necessary select a sun filter for sunny conditions. Select the automatic temperature range function of the camera.

- Take and store images and make notes of the prevailing climate conditions (alternatively have a simple logger for solar radiation, wind and ambient temperature). The images of Figure 5.8 a, b, d, e show the IR camera image and the profile the camera produces. This information is normally stored by the camera's storage device.

Evaluation procedure

- Depending on the system to be used, the evaluation of the TX factor and the calculation of the heat loss can be done on-line or off-line. The evaluation procedure involves a PC-based software for data-processing of the IR pictures and a program for calculating the TX value from the temperature profile.

– In principle the following evaluation steps have to be taken:

– *Calculation of the TX-value.* This step involves a smoothing procedure of an usually noisy TX profile and the definition of the bottom line. In this step it is important to define a bottom line and a smoothed temperature profile in order to calculate the area below the curve correctly. The principle is seen from figure 5.8.c. The dashed bottom line for the profile that has not been smoothed gives a lower basis level and results in too large TX factors. Even asymmetric profiles can be accounted for by the bottom line method. The TX area is calculated between the smoothed temperature profile and the inclined (dashed pointed) bottom line. The TX profile ends at the limits of the integration width. We made the calculations by copying the profile into a spreadsheet program on a PC (Microsoft EXCEL).

– Once a measured TX value (TX_{meas}) is determined, it together with other parameters that must be known (or estimated) are inserted in the ATXIM-equations (15) or (16) that yield the estimated heat loss, P_f

Future development

– For the future we expect that this curve smoothing and bottom line procedures can be built in as a TX option of the IR camera. Modern cameras today already include enough computing power for doing so. However an appropriate software for heat loss calculations must be developed.

– It should also be possible for the IR camera to perform the measurement of X. Optical distance measurements are common place in today's photo techniques and it should be possible to integrate a scale for the measurement at a certain distance into the IR picture.

– The remaining parameters wind, burial depth, and thermal conductivity must be treated as input parameters to the camera.

7.4 ACCURACY

The accuracy of the methods is difficult to estimate. Measurements have been performed on test fields in Studsvik (Sweden), Lyngby (Denmark), Fort Jackson (South Carolina, USA), and also in earlier field tests in Finland and Västerås (Sweden). The accuracy varied between a few percent deviations up to some 20 % when compared with heat losses measured or calculated by other means. Some of the experimental uncertainties that could have affected the agreement are the soil properties, burial depths, the wind conditions, the history of the pipe temperatures, and the uniformity of the ground surface.

It is, of course meaningful to repeat the measurements in each case a few times, especially if it is windy, in order to eliminate incidental errors. The information stored on an IR image usually covers a pipe length of 4 - 5 m. By investigating the picture, i.e. using the isotherm mode, one can determine which part of the pipe section the TX factor investigation should be performed on. If nonuniformities of the surface disturb the profile, an average over say 3 different profile positions will yield a better result.

8 Comparison of different methods for determining heat losses from pipes

8.1 INTRODUCTION

The investigation described in this chapter aims at making a comparison between different methods, including the TX-factor method, to determine the heat loss from district heating (DH) pipes. Several methods are applied on a single test object: temperature sensors, heat flux meters, thermography. The validity of interpretative models based on steady-state assumptions is also investigated.

This work was initiated with financial support from the Danish Energy Agency, from Chalmers University of Technology, from the District Heating Research Programme of the Nordic Council of Ministers as well as from the Technical University of Denmark. It received further funding from the IEA as an extension to the ongoing IEA Annex IV project ”Network Supervision”. In this chapter, a summary is presented of the work performed up to date and of the conclusions reached. A more comprehensive report is available elsewhere (Bøhm and Borgström, 1996).

Methods for determining heat losses in-situ

Bøhm (1990 and 1991) has discussed extensively the various methods that can be used to determine heat losses from DH pipes in situ. Below a short description of those methods that are used in this investigation is provided for the sake of clarity. The methods used are:

A1:	Temperature difference across the pipe insulation
A2:	Casing temperature and heat resistance of the ground
A3:	Heat flux meters on the casing
B:	Determination of the thermal conductivity of the insulation
C1:	Temperature distribution in the soil
C2:	Temperature distribution on the surface (TX-factor)
D:	Use of existing heat meters

This selection has been made with practical applications in mind.

Many parameters are needed for these methods, and it is possible to adjust these in order to obtain the best result for each method. Such an optimization will not be performed here: the same basic assumptions will be used for all methods.

Method A1: Temperature difference across the pipe insulation

The heat loss is calculated using an estimated thermal conductivity of the insulation, a temperature difference measured across the insulation and the assumption of radial heat transfer. A correction has to be made in order to take into account the influence of the neighbouring DH pipe on the heat loss. In a typical case, the thermal conductivity of the insulation is unknown and higher than it was, when the pipe was installed.

Method A2: Casing temperature and heat resistance of the ground

The heat loss is calculated using the temperature of the casing and the undisturbed ground and the steady state heat resistance of the ground (including the resistance at the surface). A correction may also be made for the neighbouring pipe.

As neither the temperature of the casing nor the temperature of the soil are uniform, a choice must be made as to where they are measured. Here, the casing temperature is measured at the top of the casing and the temperature of the undisturbed soil is measured at the same depth as the centre line of the pipe.

The resistance of the soil is directly dependent on the conductivity of the soil, thus this becomes an important parameter.

Method A3: Heat flux meters on the casing

The heat loss is calculated directly from the signal of the heat flux meter (HFM). A correction factor is used in order to take into account the heat flux distribution on the casing, the curvature of flexible HFMs, the temperature sensitivity of the thermocouples inside the HFM, and the differences in thermal conductivity between soil and HFM. For preinsulated pipes, the heat flux distribution is rather uniform and the correction for the temperature sensitivity is negligible at the actual casing temperatures. However, the difference between one-dimensional heat flux and the actual heat flux distribution cannot be disregarded. From previous work, we know that in some cases the HFM will measure only 50% of the real heat flux.

Method B: Determination of the thermal conductivity of the PUR-insulation

The thermal conductivity of the insulation is determined by measuring the heat flux through the insulation and the temperature difference across the insulation. The value determined can then be used in calculations of the heat losses.

In this investigation, equipment developed at Chalmers University of Technology (Borgström, 1994) was used. Here, soil is removed from around the DH pipe so that

the pipe is not in contact with the surrounding soil for a distance of approx. 1.5 m. The equipment, consisting of a heat flux meter and of preformed polystyrene insulation shielding the heat flux meter, is placed directly on the casing. Measurements are performed while the DH pipe is in operation.

With this method the varying properties of the material (soil) that usually surrounds the pipe are of no concern since the heat is lost by the pipe to air during the period of the determination of thermal conductivity. The shielding insulation protects the heat flux meter from radiation and convection and reduces the effect of fluctuations in the air temperature.

A detailed analysis of the errors in this method is found in (Borgström, 1994) to which the reader is referred.

Method C1: Temperature distribution in the soil

The temperature field in the soil around the DH pipes can be utilised to estimate the heat loss. Kusuda et al. (1984) used temperature measurements at pipe depth or lower, while Beck and Karnitz (1986) measured the soil temperature one foot below surface. In both cases it was assumed that steady state line source theory could be applied and that temperature fields caused by the heat losses and caused by climatic variations could be superposed. These assumptions may be questioned (Bøhm, 1990).

Method C2: Surface temperature distribution - the TX-factor

The TX-factor method is described at some length in this report. The temperature profile at the surface may be determined using temperature sensors on the surface or using an infrared camera. A TX-factor could also be computed from temperature measurements below surface, if available, although this would require a different interpretation model than that proposed here.

Method D: Utilizing existing heat meters

If heat meters are inserted in the supply and return pipes, at both ends, the actual heat loss in the section between the meters may be determined directly. However, heat meters are seldom installed this way and the information provided by SCADA (Supervisory Control and Data Acquisition) systems may be incomplete. Actually, the heat stored in the section is obtained, not the heat loss. These may be equated if a steady state condition has been established. Otherwise a dynamic heat loss method may be applied, here a revised lumped model (Bøhm, 1984).

8.2 THE EXPERIMENTAL SITE

Suitable test sites must satisfy several requirements, one of them being the possibility to use installed heat meters in order to estimate the heat losses from the DH pipe at the test site. Another requirement is that the temperature field in the ground should not be disturbed by buildings nearby, for example. Lastly, access to the site and electricity supply must be considered. A transmission pipe in the VEKS (Western Copenhagen Heat and Power Transmission Company) system connecting Langager with Solrød, a distance of approximately 4.8 km, was chosen. The exact location of the test site is in Karlstrup, 2.95 km from Langager.

The pipe layout is shown in Fig. 8.1. The pipes are 273 mm pre insulated pipes with a casing diameter of 400 mm. The pipes are buried 1.28 m below ground level (distance from pipe center line) and the distance between the center lines for the supply and return line is 0.73 m. This transmission line is approximately five years old and the insulation is in good condition.

A sketch of the test site is shown in Fig. 8.2. As this area had previously been used for growing crops, the ground below the top soil had not been disturbed except for the part excavated for laying the DH pipe. The top soil itself was 0.15 - 0.20 m deep, followed by a thick layer of moraine clay that extends below the deepest temperature sensors, 1.8 m below ground level. Samples of the soil have been collected at the site.

Figure 8.1 Scheme of the pipe system.

Figure 8.2 Test site for heat loss measurements in Karlstrup.

8.3 INSTRUMENTATION

In location A (methods A1-A3), approximately 25 m from the tool shed with the data acquisition system for this investigation, a hole was dug to the top of the pipe casings and two heat flux meters from different manufacturers were placed on each pipe. The soil was backfilled into the hole as soon as the instrumentation had been completed.

In location B (method B), close to the tool shed, the soil was removed completely from the pipes for a distance of about 3 m. A thermocouple and a heat flux meter were placed on the casing of the supply pipe and the casing was then protected using polystyrene insulation. Later, the return pipe was similarly instrumented.

In location C (methods C1-C2), the top soil was partly removed in order to allow infrared analysis of the surface. A string with eight differential thermopiles was laid out 0.4 m below the surface, perpendicularly to the center line. The thermopiles

were obtained by coupling 5 thermocouples in series in order to increase the signal. Each junction was cast in a small epoxy plate.

A similar string was placed 0.05 m below the surface. Later (5 October 1995) it was fastened underneath a 3 mm thick sheet of asphalt roofing board. This board was then placed on top the ground's surface.

The strings were laid so that the fifth thermopile was placed vertically above the centre line of the DH line. The reference junctions were placed closest to the supply pipe, see Fig. 8.1.

A vertical staff with temperature sensors (both thermocouples and thermistors at the same level) was drilled into the soil at the same spot as the reference junctions of the horizontal strings. The thermocouples were single differential thermocouples. The reference junctions were collected in a small buried isothermal container close by, the temperature of which was measured using a single thermocouple connected to the datalogger.

The soil was backfilled into the trench as soon as the instrumentation had been completed.

In spot D, approx. 15 m from the pipe, the temperature of undisturbed soil at different depths was measured using a similar staff with temperature sensors similar to that in location C.

Measurement data were collected using a HP datalogger system with built-in temperature reference. The datalogger, the thermocouple wires and the heat flux meters were calibrated previous to installation at the test site. The data logger made one series of measurements (one scan) every minute.

As it was not possible to measure the temperature of the DH water in Karlstrup, additional data were obtained from the SCADA (Supervisory Control and Data Acquisition) system in the VEKS control room. These data are 5 minutes mean values of supply and return temperatures as well as flow rates in the Langager and the Solrød heat exchanger stations. Because of design choices in the SCADA system, the resolution of the data reported by the SCADA system is not as good as that of the data actually measured.

Data acquisition started 7 September 1995, one week after the instrumentation had been completed. Until 22 September 1995, 10 minutes mean values were stored by the datalogger, and from this date one hour mean values were stored. In this report data until 5 November 1995 have been included.

The comparison between methods is made for a period of 200 hours starting on 16 September 1995. There are days without sunshine in this period and the TX-factor is stable.

8.4 THERMOGRAPHY

On 1 November 1995 an AGEMA 470 infrared system was used to measure the surface distribution across the DH-pipe at location C. The camera, mounted on a tripod, was placed for a portion of the time on a sky lift and for the remaining time on the roof of the tool shed.

TX-factors could be obtained from the surface temperature distributions. However, the profile were too flat and the TX factors too low for further analysis because of very bad weather conditions (heavy rain). An example can be seen in Figure 4.16. A new infrared survey is planned for the spring of 1996.

8.5 THEORETICAL HEAT LOSSES

The samples of soil taken at the experimental site were graded and their water content and dry density were determined. Basing on the results, we have chosen to use a low value and a high value for the thermal conductivity for the soil: 1.0 W/(m·K) and 2.5 W/(m·K) respectively in order to bracket the heat losses. Similarly, we have chosen high and low values for the heat transfer coefficient at the surface: 5.0 W/(m²·K) and 25 W/(m²·K) respectively. A value of 14.6 W/(m²·K) has previously been recommended by Kvisgaard & Hadvig (1980).

Assuming a thermal conductivity of 0.029 W/(m·K) for the insulation and using the analytical solutions, see Bøhm (1990), one obtains the theoretical heat losses shown in Table 8.1. The temperature in the supply line is 100°C, in the return line, 60°C and the soil temperature is 11°C.

Table 8.1 Theoretical heat losses for varying parameters.

λ_g	h_s	U_1	U_2	q_s	q_r
W/(mK)	W/(m²·K)	W/(m·K)	W/(m·K)	W/m	W/m
1.0	5.0	0.4274	0.0412	36.02	17.28
	14.6	0.4297	0.0391	36.33	17.57
	25.0	0.4302	0.0386	36.40	17.64
2.5	5.0	0.4737	0.0229	41.04	21.18
	14.6	0.4764	0.0203	41.40	21.53
	25.0	0.4771	0.0197	41.49	21.62

The influence of the thermal conductivity of the soil is less then 15% for the supply line and less than 25% for the return line.

8.6 RESULTS

The temperatures in the supply line and in the return line were stable, 100°C and 60°C respectively, during the whole period. However, disturbances caused by the heat production plants and heat exchanger stations were observed.

Detailed results are presented in Bøhm and Borgström (1996), thus only the main results will be reviewed here.

Dynamic heat loss model

Calculations using the two different values for the thermal conductivity of the soil yielded heat losses of 35 W/m and 40 W/m for the supply pipe and 15 W/m and 20 W/m for the return line. The transient response is very good and the result is consistent with the heat losses in Table 1.

Method A1: Temperature difference across the insulation

The heat losses are 35 W/m and 15 W/m for the supply and the return line respectively, which is also in good agreement with the theoretical values in Table 1. The thermal conductivity of the soil has little influence. The transient response of this method is very good.

Method A2: Casing temperature and heat resistance of the ground

Calculations using a value of 1.0 W/(m K) for the thermal conductivity of the soil yield heat losses of ca 23 W/m for the return line and ca 35 W/m for the supply line. Using a value of 2.5 W/(m K) yields losses of ca 60 W/m and ca 90 W/m for the return and the supply pipe respectively. If one neglects the heat losses from the neighbouring supply pipe, the heat loss calculated for the return pipe increases with 5 W/m.

The heat loss is inversely proportional to the thermal conductivity of the ground, which means that this parameter is a crucial one. The transient response is not good.

Method A3: Heat flux meters on the casing

The values of the heat loss recorded by the heat flux meters is ca 10 W/m² and ca 20 W/m² for the return and the supply pipe respectively. It appears that the multiplicative correction factor mentioned in the description of the method above should be 1.4. The transient response is very good.

Method B Determination of the thermal conductivity of the insulation

The thermal conductivity of the insulation was determined for both supply and return pipe. The temperature of the district heating water, necessary for the calculation, was obtained using the dynamic heat loss model.

The values of the thermal conductivity thus obtained are 0.0294 W/(m·K) and 0.0287 W/(m·K) for the supply and the return pipes respectively. Therefore, a value of 0.029 W/(m·K) was used in this study.

Method C1: Soil temperature distribution

Using temperature measurements deep into the ground, one obtains a total heat loss between 100 and 140 W/m if the thermal conductivity of the soil is 2.5 W/(m·K) and between 40 and 80 W/(m·K) with a value of 1.0 W/(m·K). The heat loss is very dependent on the conductivity.

The three temperature sensors closest to the surface showed an influence from the daily weather variations. Using data obtained at 0.4 m depth and the two values of the thermal conductivity of the soil, one can calculate a total heat loss of 35 W/m and ca 75 W/m respectively.

In both cases, the transient response is bad.

We attempted to separate the heat loss in the return pipe from that in the supply pipe using a double set of differential temperatures. This was not successful: we obtained a negative heat loss for the return pipe.

Method C2: Surface temperature distribution

In the same way as the TX-factor is calculated for the surface, a TX-factor can be calculated for any level below the ground surface. The influence of thermal conductivity of the soil and surface heat transfer coefficient is large. Using the temperature data at 0.4 m level below surface one obtains a total heat loss between approximately 50 W/m and about 130 W/m depending on which combination of values in Table 1 one uses. The transient response is not good.

We attempted to separate the heat losses using the TX-factor 0.4 m below ground and one deep differential temperature measurement. This was not successful: we sometimes obtained a larger heat loss for the return pipe than for the supply pipe.

The TX-factor obtained from temperature measurements 0.05 m below surface are shown in Figure 8.3. It should be observed that, when the incident solar radiation increases in the second half of the 200 hours period, the TX-factor starts to oscillate. This could also be observed in data from the 0.4 m level, but to much less extent.

Unfortunately, the TX-profile obtained using the infrared camera on 1 November 1995 was too flat for analysis because of the heavy rain.

However, using information from the temperature sensors, one can estimate that a value of 2.0 K m should be representative for the TX-factor in periods of low wind and solar radiation. Disregarding the transient terms and the influence of the wind, one then obtains the following values of the heat loss when using the equation in Jönsson & Zinko (1993):

q_{total} = 67.2 W/m for a thermal conductivity of 1.0 W/(m·K)

and q_{total} = 70.7 W/m for a thermal conductivity of 2.5 W/(m·K)

Method D: Using existing heat meters

The flow rate of water in the transmission line shows a clear daily variation, from ca 30 m³/h to 90 m³/h on a typical day. Filtering the data, one obtains a mean heat loss of 42.1 W/m from the supply line and of 11.6 W/m from the return line. The total heat loss is thus 53.7 W/m. The total heat loss is less affected by an absolute error of the temperature sensors in the heat exchanger stations than the separate heat loss from the supply line and the return line, respectively.

Figure 8.3: TX factor and differential temperatures measured with thermocouples 5 cm below ground surface.

8.7 SUMMARIZING REMARKS

The methods for determining heat losses in situ differ with regard to:

- time consumption and costs of applying the specific method
- demand on accuracy of temperature measurements
- sensitivity to computational parameters, e.g. the thermal conductivity of the ground
- response to transients
- assumptions in the model used in the interpretation

Conclusions which may be drawn from this study are (the transmission line being in a good thermal condition):

Method A: Temperature difference across the pipe insulation works very well. A correction term has been introduced in order to obtain the true steady state heat loss, taking into consideration the influence of the neighbouring pipe. The transient response is good because the PUR-insulation has little thermal capacity. When combined with method B the thermal resistance of the PUR insulation can be calculated. The method will probably not work very well for DH pipes in poor conditions and for non-radial heat transfer (DH ducts).

Method A2: Casing temperature and heat resistance of the ground is very dependent on the thermal conductivity of the ground, a quantity which is difficult to measure or calculate because of varying moisture content in the soil and probably non uniform conditions in the ground.

Method A3: Heat flux meters on the casing has a very good transient response and the heat flux meters are easy to install. It appears necessary to calibrate them in realistic conditions, i.e. not in one-dimensional conditions. The method is very accurate for pre insulated pipes. The correction factor was ca 1.4 in our case.

Method B: Determination of the thermal conductivity of the PUR-insulation" works well. However, the method is costly and time-consuming because the soil around the pies must first be removed and later backfilled. For pre insulated pipes (with radial heat transfer) the method is very accurate.

Method C1: The best results for "Soil temperature distribution" were obtained from measurements at a depth, where the temperature of the soil

changes slowly. The method is very dependent on an accurate value of the thermal conductivity of the soil. It was not possible to separate the total heat loss into heat losses for each pipe. This is not in agreement with findings of previous work, in which measurements one foot below the ground surface was used with fairly good result. However in the case of a much larger heat loss.

Method C2: Surface temperature distribution - the TX-factor - was tested with three different procedures to obtain the TX-factor. The measurements are difficult to carry out with temperature sensors at the surface and they seem to be affected by a time lag in the vertical transfer of heat. Furthermore, the factor becomes unstable when solar radiation or wind is strong. Elsewhere in this report we have demonstrated that a TX-factor is best obtained from infrared measurements. However in the case of measurements at a particular day, heavy rain had flattened the TX profile.

A TX-factor determined 0,4 m below the surface is much more stable, but the instrumentation is more costly and more time consuming. Also, the heat loss calculated from the TX-factors in this case is influenced by the choice of thermal conductivity for the soil and by the coefficient of heat transfer at the surface. The heat loss obtained from the equation in Jönsson and Zinko (1993) is 10% to 25% larger than the heat loss obtained from the analytical solutions, see Table 1.

Method D: The Application of existing heat meters is very much dependent on specific conditions at the site and the accuracy of meters and temperature sensors. In the case of the Langager-Solrød line, strong daily variations in the flow rate made it difficult to calculate the steady state heat loss from any of the suggested equations, even if the signals were filtered. The mean heat losses for September 1995 are consistent with the analytical expressions.

Finally, it should be stated that the transmission line is in a good thermal condition so that the heat loss could be obtained from the analytical expressions. To determine the real heat losses more accurately, the temperature sensors in Langager and Solrød must be recalibrated and additional geotechnical analyses must be carried out.

9 Conclusions and recommendations

The following conclusions and recommendations can be drawn from our findings:

- The proposed model for quantitative termography analyses has been shown to expand the range of applicability of conventional thermography evaluation. The TX model represents a possibility for the quantitative (instantaneous) determination of heat losses from buried pipes.

- Thermography during exposure to long wave and solar radiation is possible if the surface is uniformly exposed to the radiation and if it has a uniform emissivity within the surface area to be analyzed. The TX model can be applied under suitable conditions at both day and night.

- It has been shown that the wind has a very strong influence on the instantaneous TX factor. It is included in the Advanced TX Interpretation Model ATXIM. The ATXIM includes wind conditions during the last 7 hours before the thermography measurements. The model is verified for wind speeds up to 10 m/s.

- Rain conditions and wet and drying surfaces as well as frost in the ground are not suitable for quantitative heat loss analysis using the TX method.

- The following parameters are included in the ATXIM: Average wind speed over the last 7 hours, the thermal conductivity of the ground, the burial depth of pipes h_f, and the integration half width X.

- Factors that can be optionally included are the changes of the surface temperature during the last 5 hours and of the pipe temperature during the last week.

- The thermal conductivity of the soil has - in contrast to a common opinion - only a relative small influence on the heat loss. The exact soil composition and the value must not be known precisely for determining the heat loss.

- Experimental verification of the model included a depth h_f of 1.1 m and an integration width 2X up to 5 m. The burial depth of the buried pipes is an important parameter and should be known as closely as possible.

- The physical properties of the surface layer and the surface itself, as well as the irradiation, must be uniform.

- Asphalt shingles were shown to be useful as a reference cover on non uniform surfaces or surfaces with undefined physical properties.

- The TX model cannot be applied on grass surfaces and uneven surfaces.
- The error of the model should under suitable conditions be within ± 20%.
- We recommend further evaluation of the application of TX model as expressed by the ATXIM in the course of practical field thermography surveys in order to develop the procedure for a camera-integrated TX option.

10 Literature

BARTSCH, D.
Search for Leaks in District Heating Systems (Fernvärmeversorgung Niederrhein, Dinslaken, Germany) Fernwärme-Int., Feb 1979, ISSN: 0340-2572.

BECK, J.V. and KARNITZ, M.A.
Parameter estimation study of heat losses from underground steam pipelines. ORNL/TM-9928. Oak Ridge National Laboratory. 1986.

BENONYSSON, A.
Dynamic modelling and operational optimization of district heating systems. Ph.D. Thesis. Laboratory of heating and air conditioning, Technical University of Denmark. 1990.

BORGSTRÖM, M.
Determination of the thermal conductivity of the insulation in district heating mains, Field measurements. Doctor of engineering thesis. Department of building physics, Chalmers University of Technology, 1994, Göteborg, Sweden.

BIGL, S. R., HENRY, K. S., and ARCONE S. A.
Detection of buried utilities. Review of available methods and comparative field study CRREL Report 84-31, Dec 1984.

BØHM, B.
Dynamiske temperaturforløb i fjernvarmeledninger, (Dynamic temperature response in district heating pipes).1984, Teknologisk Institut. ISBN 87-7511-387-2.

BØHM, B.
Enkle metoder til bestemmelse af varmetab fra fjernvarmeledninger under normal drift, (Simple methods for determining the heat loss from district heating pipes under normal operating conditions). 1990, Laboratory of Heating and Air Conditioning, Technical University of Denmark. ISBN 87-88038-18-1.

BØHM, B.
Determination of heat losses from district heating networks. Report 3.15E, 25. 1991, UNICHAL Congress, Budapest.

BØHM, B. and BORGSTRÖM, M.
A comparison of different methods for in-situ determination of heat losses from district heating pipes. 1996, Centre for District Heating Technology, Technical University of Denmark.

HANSEN, K-E.
Fjernvarme 32. Termografering af fjernvarmeledninger (District heating 32. Thermography of district heating culverts). Danske fjernvarmevaerkers forening, April 1987.

LJUNGBERG, S. Å.
Termografering av fjärrvärmenät, Västeråsprojektet, en metodstudie. (Thermography of District Heating Networks, the Västerås project, a method study). Värmeverksföreningen och Statens Institut för Byggnadsforkning, Dec 1987.

JONASSON, U. and STÅLHANDSKE, H. Metoder att minska värmeförluster i befintliga fjärrvärmesystem, Etapp 2. Rapport R23:1986, Byggforskningsrådet, Sverige, ISBN 91-540-4544-4.

JÖNSSON, B. and ZINKO, H.
Quantitative heat loss analysis of heat and coolant distribution pipes by means of thermography. IEA District Heating, 1992, ISBN 90-72130-35-9.

KUSUDA, T., FANG, J.B. and ELLIS , W.M.
A method for estimating heat loss from underground heat distribution systems. National Bureau of Standards, ASTM Symposium on thermal insulation, materials and systems, 1984, Dallas, Texas.

KVISGAARD, B. and HADVIG, S.
Varmetab fra fjernvarmeledninger, (Heat loss from pipelines in district heating systems, 1980, Teknisk Forlag.

MØLLER JENSEN J. and LUND, H.
Design Reference Year DRY - Et Nyt Dansk Referenceår (A New Danish Reference Year). Meddelelse nr. 281. Oktober 1995. Laboratoriet for Varmeisolering, DTU.

PERERS, B., JÖNSSON, B.
Värmeförluster i fjärrvärmenät med termografi. (Heat loss measurements in district heating networks by means of thermography). Studsvik AB, Sweden 1990. Studsvik/ED-90/28.

PERERS, B., SCHMELING, P.
Bestämning av värmeförluster i fjärrvärmenät med termografi. Simuleringsmodell för noggrannare bildanalys. (Determination of heat leaks in District Heating Systems by means of thermography). Studsvik AB, Sweden 1989. Studsvik/ED-89/5.

PHETTEPLACE, G., CARBEE, D. and KRYSKA, M.
Field Measurement of Heat Losses from Three Types of Heat Distribution Systems, U.S. Army Cold Regions Research and Engineering Laboartory, Hanover, NH, SR 91-19, (November 1991).

PHETTEPLACE, G.

Measurement of heat losses from a buried heat distribution system. HTD-Vol. 172, Heat Transfer in geophysical media. 1991, ASME.

PHETTEPLACE, G.
Measurement of heat losses from an operating district heating system. FWI, Jg. 21, 1992,
Heft 3.

SJÖBERG, P.
Användarmanual för Kulvertförlust - Simuleringsprogram.
(User manual for a program for the simulation of pipe losses, part of master thesis).
University Västerås, October 1988.